

**Investigation of Heterogeneous Reactions
of ClONO_2 , HCl , and HOCl on Liquid Sulfuric Acid Surfaces**

Renyi Zhang*, Ming-Taun Leu*, and Leon F. Keyser

Earth and Space Sciences Division

Jet Propulsion Laboratory

California Institute of Technology

Pasadena, California 91109

(Submittal to *J. Phys. Chem.*, August 18, 1994)

* To whom correspondence should be addressed

Abstract

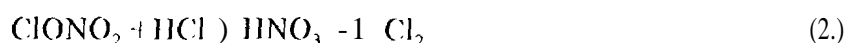
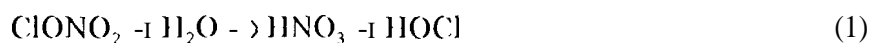
The heterogeneous reactions of $\text{ClONO}_2 + \text{H}_2\text{O} \rightarrow \text{HNO}_3 + \text{HOCl}$ (1), $\text{ClONO}_2 + \text{HCl} \rightarrow \text{Cl}_2 + \text{HNO}_3$ (2), and $\text{HOCl} + \text{HCl} \rightarrow \text{Cl}_2 + \text{H}_2\text{O}$ (3) on liquid sulfuric acid surfaces have been studied using a fast flow-reactor coupled to a quadrupole mass spectrometer. The main objectives of the study are to investigate a) temperature dependence of these reactions at a fixed H_2O partial pressure typically in the lower stratosphere, b) relative importance or competition between reactions 1 and 2, and c) the effect of HNO_3 on the reaction probabilities due to the formation of a $\text{H}_2\text{SO}_4/\text{HNO}_3/\text{H}_2\text{O}$ ternary system. The measurements show that all the reactions depend markedly on temperature at a fixed H_2O partial pressure: they proceed efficiently at temperatures near 200 K and much slower at temperatures near 220 K. The reaction probability (γ_i) for ClONO_2 hydrolysis approaches 0.01 at temperatures below 200 K, whereas the values for γ_2 and γ_3 are on the order of a few tenths at 200 K. Although detailed mechanisms for these reactions are still unknown, the present data indicate that the competition between ClONO_2 hydrolysis and ClONO_2 reaction with HCl may depend on temperature (or H_2SO_4 wt %): in the presence of gaseous HCl at stratospheric concentrations, reaction 2 is dominant at lower temperatures (< 200 K), but reaction 1 becomes important at temperatures above 210 K. Furthermore, reaction probability measurements performed on the $\text{H}_2\text{SO}_4/\text{HNO}_3/\text{H}_2\text{O}$ ternary solutions do not exhibit noticeable deviation from those performed on the $\text{H}_2\text{SO}_4/\text{H}_2\text{O}$ binary system, suggesting little effect of HNO_3 in sulfate aerosols on the ClONO_2 and HOCl reactions with HCl . The results reveal that significant reductions in the chlorine-containing reservoir species (such as ClONO_2 and HCl) can take place on stratospheric sulfate aerosols at high latitudes in winter and early spring, even at temperatures too warm for polar stratospheric clouds (PSCs) to form in regions where nucleation of PSCs is sparse. This is particularly true under elevated sulfuric acid loading, such as that after the eruption of Mt. Pinatubo.

Introduction

It is now well established that heterogeneous reactions occurring on the surfaces of polar stratospheric cloud particles play a central role in the ozone depletion.¹ The surface-catalyzed reactions convert chlorine-containing reservoir species into photochemically reactive forms, leading to high rates of ozone destruction by active chlorine species, Cl and ClO. Of equal importance to the polar stratospheric ozone depletion is the concomitant removal of nitrogen oxides from the gas phase, which inhibits the formation of chlorine nitrate and subsequently leads to large concentrations of ClO. Such heterogeneous processing of reservoir chlorine species on PSC particles has been clearly seen in recent field observations, showing chemical changes such as the increase in ClO and concurrent decreases in HCl, ClONO₂, and ozone as measured from inside to outside of the chemically perturbed regions in Antarctica and the Arctic.²⁻⁵ Furthermore, laboratory studies have documented that these heterogeneous reactions proceed efficiently on the PSC materials,⁶ which are believed to consist of either nitric acid hydrates (type I) or ice (type II).^{7,8}

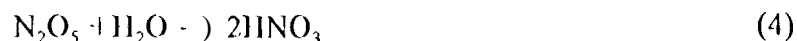
Similar reactions occurring on stratospheric sulfate aerosols have also been proposed to have a significant effect on the chemistry of the global stratosphere.⁹⁻¹¹ The sulfate aerosol layer, which exists at latitudes between 10 and 30 km, is composed of aqueous sulfuric acid particles with a mean diameter of about 0.1 μm and concentration from 1 to 10 cm^{-3} under unperturbed stratospheric conditions. Major volcanic eruptions, such as the eruption of Mt. Pinatubo, may significantly increase the particle size and concentration. Steele et al.¹² first compiled the sulfate aerosol compositions as a function of temperature, predicting an aerosol concentration of 70-80 wt % at mid-latitudes and of less than 50 wt % at high latitudes. Recent studies¹³⁻¹⁶ have suggested that, at lower temperatures such as those prevailing in the early polar winter, the sulfate aerosols absorb a significant amount of HNO₃, leading to the formation of a H₂SO₄/HNO₃/H₂O ternary system prior to the onset of PSCs. Additionally, on the basis of laboratory observations, crystalline sulfuric acid hydrates such as tetrahydrate and hemihexahydrate^{17,18} or monohydrate¹⁹ have been proposed to form and persist in certain stratospheric regions.

The heterogeneous reactions, which could promote chlorine activation and affect the stratospheric NO_x budget, are as follows:



On crystalline sulfuric acid tetrahydrate, reactions 1 to 3 have been shown to proceed efficiently at low temperatures ($< 200 \text{ K}$).^{24,25} Earlier volatility studies²⁶ reported a negligible amount of HCl in liquid sulfate aerosols, too small for reactions 2 and 3 to occur at significant rates on the global stratosphere. In addition, other laboratory studies yielded very small uptake coefficients for these reactions on liquid sulfuric acid solutions.^{22,27} It is now clear that the rates of these two reactions are critically determined by the amount of HCl dissolved in the liquid solutions, which, in turn, depends on both temperature and aerosol acid content. Thus, changes in stratospheric temperatures (which will also change the sulfate aerosol concentration) would likely result in highly non-linear behavior for these two reactions. Recent laboratory results predict an equilibrium HCl concentration as high as 0.1% by weight in the stratospheric sulfate aerosols at temperatures below 192. K and at an HCl mixing ratio of a few ppbv,¹⁵ an amount which would be consistent with reaction probabilities on the order of a few tenths for reactions 2 and 3.³ More recently, efforts have been made to calculate reaction probabilities based on laboratory measured quantities;^{28,29} a theoretical framework has been proposed to apply the laboratory data to the stratosphere. Chemical processing of air by stratospheric sulfate aerosols via reactions 2 and 3 at high latitudes is supported by recent AASE II observations,¹⁴ which reveal a significant depletion in both ClONO_2 and HCl column abundances in the Pinatubo plume, even when there is no PSC signature.

Another important heterogeneous reaction on liquid sulfate aerosols is



This reaction is believed to reduce the stratospheric NO_x concentration and consequently result in an increase in the abundances of ClO and O₃. Several laboratory results have concluded that the reaction probability for reaction 4 is independent of temperature, sulfuric acid concentration, and even particle size, with a value of about 0.1.^{20, 23} There is now accumulating evidence that the observed abundance of nitrogen and chlorine species in mid-latitudes cannot be simulated accurately in numerical models by gas phase processes alone, but that inclusion of N_2O_5 hydrolysis produces better agreement between observations and calculations. Conversely, the

proposed formation of solid sulfuric acid particles in the stratosphere could potentially suppress the N_2O_5 hydrolysis and thus terminate this reaction channel.^{19,24}

The aim of this work is to perform direct laboratory experiments on liquid sulfuric acid surfaces under stratospheric conditions. The reaction probabilities for ClONO_2 hydrolysis and HCl reactions with ClONO_2 and HOCl at the reactant concentrations characteristic of the lower stratosphere have been measured. The temperature dependence of these reactions was investigated at a fixed H_2O mixing ratio of about 5 ppmv and at temperatures from 195 to 220 K. The relative importance or competition between the hydrolysis of ClONO_2 and the ClONO_2 reaction with HCl was also examined so that accurate chlorine activation processes in the stratospheric sulfate aerosols can be applied and simulated in atmospheric models. Finally, we investigated the effect of HNO_3 on the reaction probabilities due to the formation of the ternary $\text{H}_2\text{SO}_4/\text{HNO}_3/\text{H}_2\text{O}$ system, which has been proposed to occur prior to the onset of type 1 PSCs.

Experimental Approach

Reaction probability measurements were performed in a fast flow reactor attached to a differentially pumped quadrupole mass spectrometer. The reactor section is shown schematically in Figure 1. An overview of the experimental procedure is given here, and details of the apparatus have been discussed elsewhere.³⁰

The flow reactor, of inner diameter 2.8 cm and length 34.0 cm, was horizontally-mounted and had three movable injectors located at the upstream end. A jacketed injector (1.0-cm o.d.) kept warm by circulating a room temperature solution of ethylene glycol in water was used to add H_2O and HNO_3 to the system. Normally, this injector was positioned near the upstream end to prevent possible warming of the substrate. The reactants (such as ClONO_2 or HOCl) were introduced through a centrally-located unjacketed injector (0.3-cm o.d.), and a third unjacketed injector of similar o.d. was used to introduce HCl . All the gaseous species were delivered to the flow tube along with small He flow ($0.1\text{--}5.0\text{ cm}^3\text{ min}^{-1}$ at STP) and further diluted in the main He flow ($280\text{ cm}^3\text{ min}^{-1}$ at STP) before contacting the liquid surface. Typically, the flow reactor was operated at 0.5 Torr total pressure and 890 cm/s flow velocity.

Liquid H_2SO_4 films were prepared by totally covering the inside walls of the flow tube

with sulfuric acid solutions. To ensure a uniform wetting, the flow tube was first cleaned with a dilute HCl solution and then rinsed with distilled water. At low temperatures (< 220 K) the solutions were sufficiently viscous to produce an essentially static film which lasted over the time scale of the experiments. The thickness of the liquid was estimated to be ~ 0.1 mm.

The sulfuric acid content initially used was less than 70 wt% to avoid possible freezing of the film at temperature above 220 K. During the course of the experiments, the acid content can be varied by addition of H_2O through the jacketed injector; once exposed to H_2O , the sulfuric acid film took up H_2O and became more dilute until equilibrium was reached. Alternatively, compositional changes of the film can be made through evaporation of H_2O , by raising the flow tube temperature and by flowing dry helium over the sample. Critical parameters for the measurements were temperature and H_2O partial pressure, which determined the H_2SO_4 content (the temperature and H_2O partial pressure in the flow tube were used to estimate the acid content from the vapor pressure data of Zeleznik³¹ and Zhang et al.,¹⁸). For most experiments reported here, the H_2O partial pressure was closely maintained at $\sim 3.8 \times 10^{-4}$ Torr (corresponding to 5 ppmv H_2O mixing ratio at 100 mb in the stratosphere) while the temperature was regulated from 195 to 220 K. This was equivalent to changing H_2SO_4 content from 45 to 70 wt%. Thus, by using H_2O partial pressures similar to those found in the stratosphere, the liquid film had compositions representative of stratospheric sulfate aerosols. Frequently, the film crystallized upon further cooling below 195 K.

For measurements of reactive uptakes of ClONO_2 and HOCl on sulfuric acid due to the reactions with HCl , the acid film was first exposed to HCl vapor before introducing the reactant. In these measurements, it was important to ensure the equilibrium of HCl between the gas and liquid. This can be verified by pulling the HCl injector upstream while monitoring the HCl signal recovery in the mass spectrometer. Also, the gaseous HCl concentration had to be effectively maintained to offset changes in temperature or in H_2SO_4 content induced by addition or evaporation of H_2O . Similarly, HNO_3 was also introduced from the gas phase and allowed to equilibrate with the liquid.

Reaction probabilities (γ 's) were calculated from first-order rate constants obtained from the reactant loss or product growth. The surface area of sulfuric acid films was assumed to be the geometric area of the flow tube. Standard cylindrical flow tube analysis technique were

used.³² Corrections for gas-phase diffusion were made by using the method developed by Brown.³³ The diffusion coefficients of ClONO_2 , HOCl , and HCl were estimated using the method described by Marrero and Mason;³⁴ the values were 176 , 215 , and $296 \text{ Torr cm}^2 \text{ s}^{-1}$ for ClONO_2 , HOCl , and HCl at 200 K , respectively. A temperature dependence of $1/T^{1.75}$ was employed. The Brown correction was approximately 10% for small γ values ($\gamma < 0.01$) and as large as a factor of 4 for large values ($\gamma > 0.2$).

ClONO_2 was synthesized by the reaction of Cl_2 with N_2O_5 ,³⁵ and was eluted from a trap at 192 K through a metering valve with a He flow of $0.1 - 5.0 \text{ cm}^3 \text{ min}^{-1}$ at STP. In calibrating ClONO_2 , He was flowed through the ClONO_2 sample kept at 144 K and the ClONO_2 concentration in the flow tube was estimated by assuming full saturation of the He flow when it exited the ClONO_2 trap. HOCl was produced by passing ClONO_2 through a $40 \text{ wt } \%$ H_2SO_4 solution at 273 K . This source was stable during the experiment and contained few impurities. The HOCl concentration was estimated by its production from reaction 1 on a liquid H_2SO_4 film. For this case, a stoichiometric ratio of unity was assumed for HOCl formed due to ClONO_2 lost (justification is given below). HCl was added to the flow tube from a dilute mixture in He ($0.1 - 5.0 \%$), and its concentration was determined either by observing the pressure rise in the flow tube upon its addition or by using a $10 \text{ cm}^3 \text{ min}^{-1}$ (at STP) mass flow meter. HNO_3 was collected from a $3:1$ solution of H_2SO_4 ($96 \text{ wt } \%$) and HNO_3 ($70 \text{ wt } \%$) and was calibrated similarly to HCl . Water signals were calibrated by depositing an ice film and using its vapor pressure over the temperature range of $190 - 230 \text{ K}$.³⁶

HCl , HOCl , and Cl_2 were monitored at their parent peaks of 36 , 52 , and 70 , respectively. ClONO_2 and HNO_3 were both detected at $m/e = 46$ which corresponds to the NO_2^+ ion fragment. Detection limits were about $5 \times 10^{-8} \text{ Torr}$ for ClONO_2 , Cl_2 , HOCl , and HNO_3 and $1 \times 10^{-7} \text{ Torr}$ for HCl . These detection sensitivities were limited mainly by background partial pressures. During the experiments, all the relevant mass spectrometer signals were simultaneously recorded by using a computer data acquisition system.

Results

Observations of Physical Uptake of HCl , HOCl , and HNO_3 on a Liquid Sulfuric Acid

Because HCl and HNO₃ were added to the liquid sulfuric acid films by allowing the acid surface to equilibrate with the vapors introduced with the carrier gas, it was essential to understand their adsorption behavior on H₂SO₄ over the temperature and acid content range investigated. Also, HOCl formed by the reaction of ClONO₂ with H₂O may be retained in the H₂SO₄ solution, possibly affecting the γ values determined. Furthermore, for the HOCl reaction with HCl, the physical uptake of HOCl in H₂SO₄ solution needs to be excluded when deducing γ 's based on the HOCl loss. As a result, some direct measurements of HCl, HOCl, and HNO₃ uptakes from the gas phase were carried out. These measurements also provide information on the time scale for reaching gas and liquid phase equilibrium.

To perform the uptake experiment, a steady-state flow of the adsorbed gas was first established through one of the injectors pushed in just passing the liquid sulfuric acid film (the jacketed injector was only used for HNO₃). The injector was then quickly pulled upstream exposing a section of the film to the vapor while monitoring its mass spectrometer signal. Examples of these results are shown in Figure 2. At a H₂O partial pressure of $\sim 3.8 \times 10^{-4}$ Torr, in Figure 2(a), a 10-cm length of sulfuric acid film was exposed to HCl at 2 rein; the HCl concentration in the gas phase fell instantly upon pulling the injector and then returned to its original value as the film was saturated with HCl. At this point, no further uptake was observed, suggesting that an equilibrium had been reached between the gas and liquid. At 4 min, the injector was pushed back, resulting in a similar, yet opposite peak due to HCl desorption. Both the adsorption and desorption occurred on a time scale of less than a minute. An HCl partial pressure of 5×10^{-7} Torr was used in this experiment. In sulfuric acid, HCl undergoes dissociation, dependent on the acidic content;³⁷ its reactive form is likely to be Cl⁻.

Plotted in Figure 2(b) is the HOCl signal as it evolved with time due to exposure of a 10-cm length sulfuric acid film at the HOCl partial pressure of 1×10^{-7} Torr. This uptake is qualitatively similar to that for HCl. Though a weak acid, HOCl also dissociates in highly acidic H₂SO₄ solutions.¹⁶ As can be concluded from Figure 2(b), so long as sufficient time is allowed to saturate the acid film, reaction probabilities for the ClONO₂ hydrolysis (or HOCl reaction with HCl) can be accurately derived based on the HOCl growth (or decay).

In contrast, HNO₃ uptake by the 10-cm H₂SO₄ film was substantial (Figure 2(c)); it took about 45 min to reach saturation for the HNO₃ partial pressure of 5×10^{-7} Torr. As shown in

Figure 2(c), the slow recovery in HNO_3 after the initial drop is most likely controlled by interfacial mass transport or by liquid-phase diffusion. The significant uptake of HNO_3 by sulfuric acid is consistent with the formation of a $\text{H}_2\text{SO}_4/\text{HNO}_3/\text{H}_2\text{O}$ ternary system at this temperature, as noted in the introduction section. The extent of HNO_3 dissociation in sulfuric acid is also dependent on acidity.³⁸

Both the absorption and desorption curves, as displayed in Figure 2, can be applied to extract information such as the product of the Henry's law solubility constant (H) and square root of the liquid-diffusion coefficients ($D_l^{1/2}$). For example, the values in Figure 2 correspond to 25 and 41 (in the units of $\text{M atm}^{-1} \text{ cm s}^{-1/2}$) for HCl and HOCl . Over the few measurements taken in this work, the results are generally in good agreement with those reported by Hanson and Ravishankara.³⁸

As expected, at a given H_2O partial pressure, we have observed drastic increases in the uptake with decreasing temperature, indicating very strong negative temperature dependencies. For conditions similar to those in Figure 2(a), the time scale for HCl saturation (i. e., the time for the signal to return to its initial level) was as long as about 15 minutes at 195 K, whereas the HCl uptake was undetectable at 220 K. In general, solubilities of these species in H_2SO_4 increase with decreasing temperature at a given acid content and increase with decreasing H_2SO_4 content at a given temperature. Since the H_2O partial pressure was held constant in our experiments, temperature dependencies of these uptakes were actually two fold: at low temperatures the solubilities increased due to both decreasing temperature and decreasing H_2SO_4 content.

It should be pointed out that here we examine only the qualitative behavior of these uptake phenomena in terms of relevance to the present work. Detailed studies have been reported by Hanson and Ravishankara.³⁸

Reaction of ClONO_2 with H_2O

We have performed direct measurements of uptake coefficients for ClONO_2 on liquid sulfuric acid films at temperatures between 195 and 220 K and at a H_2O partial pressure of $\sim 3.8 \times 10^{-4}$ Torr. Reaction probabilities (γ_r) were obtained by observing the decay of ClONO_2 or the growth of HOCl as a function of injector position as it was pulled successively upstream over

the acid film.

A typical result of reactive uptake of ClONO_2 by sulfuric acid solution is shown in Figure 3 as time evolution of ClONO_2 and HOCl signals. The experiment was performed at 199 K and at a ClONO_2 partial pressure of 1×10^{-7} Torr. At -2 rein, a 1.0-cm length of H_2SO_4 film was exposed to ClONO_2 by pulling the injector upstream, and the signal of ClONO_2 dropped sharply to a very small value while the HOCl signal rose; at ~ 9.2 rein, the injector was moved back downstream to stop the exposure and both the ClONO_2 and HOCl signals returned to their initial levels. The HOCl signal is found to exhibit a noticeable delay of about a minute and half when the injector was positioned both upstream and downstream, consistent with the above-mentioned uptake behavior. As displayed in the figure, the product that leaves the surface is identified as HOCl ; the other product, HNO_3 , is left behind on the film since it is very soluble in the cold sulfuric acid solutions.¹⁵ In all of our experiments of this type, the maximum signal due to HOCl was always comparable to the initial ClONO_2 signal. Because the relative detection sensitivity of the mass spectrometer for the two molecules was approximately the same, the measurements suggest that ClONO_2 reacting with H_2O on liquid sulfuric acid yields one HOCl .

In addition to the ClONO_2 reaction with H_2O , some loss of ClONO_2 may be related to its physical uptake by sulfuric acid. In our experiments, however, it is virtually impractical to separate the two processes. Nevertheless, this should have a negligible effect on the γ measurements, because we obtained essentially the same γ 's based on both ClONO_2 decay and HOCl growth, as discussed below. Hanson and Ravishankara²⁹ reported a solubility constant of about 103 M atm^{-1} for ClONO_2 in a 60% H_2SO_4 solution at 202 K.

Figure 4 is a semi-log plot of measured ClONO_2 and HOCl signals versus injector position for an experiment performed at 199 K and at an initial ClONO_2 partial pressure of 1.2×10^{-7} Torr. The slope of the ClONO_2 decay line yields the first-order rate coefficient. The nearly-constant concentration for $110 \sim 1$ at larger injector distance can be viewed as an asymptotic value. Hence a plot of $\log(S_{\text{HOCl}}(\infty) - S_{\text{HOCl}}(z))$ versus injector distance (where z is the injector position and $S_{\text{HOCl}}(\infty)$ is the asymptotic HOCl signal at large injector distance, estimated visually from the figure) should be linear (Figure 4(b)). The slope of such a plot also yields a first-order rate coefficient. Both the ClONO_2 decay and HOCl growth validate the first order kinetics. These coefficients lead to reaction probabilities of 0.010 and 0.012 corresponding to the ClONO_2 decay

anti HOCl growth, respectively. Note that the reaction probability obtained from the HOCl growth is very sensitive to the determination of the asymptotic value of $S_{\text{HOCl}}(\infty)$. For smaller reactive uptake of ClONO_2 (i.e., at high temperatures), a longer injector distance is needed to derive its value.

In Figure 5, values of γ_1 calculated from experiments such as those displayed in Figure 4 are presented as a function of temperature using $P_{\text{ClONO}_2} = 8 \times 10^{-8}$ to 2×10^{-7} Torr. The open circles denote γ_1 's obtained from the ClONO_2 decay and the solid ones are based on the HOCl growth. The solid line is a polynomial fit through the data; the coefficients are summarized in Table 1 along with the experimental conditions. The estimated error limit of the γ_1 values is approximately $\pm 30\%$, which includes the uncertainties in measuring the first-order rate constant and in correcting for gas-phase diffusion.

It can be shown in the figure that, as the temperature varies from 220 to 196 K, γ_1 changes from about 3×10^{-4} to 0.03, increasing by two orders of magnitude. At the same time, the H_2SO_4 film is diluted from about 70 wt% to less than 50 wt%. Thus, the ClONO_2 hydrolysis shows a strong dependence on sulfuric acid content, in contrast to N_2O_5 .²⁰⁻²³ Also, these measurements do not discriminate the effects of surface versus bulk reactions and represent only the overall process. For stratospheric applications, however, the measured γ 's need to be corrected for the finite dimension of the sulfate aerosols; this will be discussed in a later section.

Reaction of ClONO_2 with HCl

We investigated the reactive uptake of ClONO_2 by liquid H_2SO_4 in the presence of HCl vapor (γ_2): the measurements were performed by first allowing the substrate to equilibrate with HCl vapor introduced into the flow tube with 1 le through one of the unjacketed injectors.

Figure 6 shows the temporal profiles of ClONO_2 , Cl_2 , HOCl, and HCl signals for a typical experiment conducted at 202 K. The initial partial pressures of ClONO_2 and HCl for this experiment were 1×10^{-7} and 5×10^{-7} Torr, respectively. At 1 min the ClONO_2 injector was pulled upstream by 3 cm and a pronounced time-independent drop was observed in the ClONO_2 signal while the Cl_2 signal rose immediately. When the injector was pushed back to its starting position at 2.6 min, both ClONO_2 and Cl_2 returned quickly to their original levels. During this process,

the gaseous HCl concentration also decreased due to the reaction, albeit to a lesser extent. No release of HOCl into the gas phase was observed. Correcting the measured ClONO₂ and Cl₂ signals for their relative sensitivities gave a yield of near unity for Cl₂.

In a separate experiment, the reaction of ClONO₂ with dissolved HCl was studied at excess ClONO₂ (Figure 7). (The initial partial pressures of ClONO₂ and HCl were 6.5×10^{-7} and 3×10^{-7} Torr, respectively.) In this case, the gas-phase HCl dropped immediately to zero upon exposure, accompanied by a pronounced decline in ClONO₂. An important difference between Figures 6 and 7 is that with higher ClONO₂ partial pressures both Cl₂ and HOCl are liberated into the gas phase. It is also interesting to note that the rise of the HOCl signal had a noticeable delay upon the exposure, whereas the fall of Cl₂ and the rise of HCl were delayed when the exposure was ended. These delays are likely due to the reaction of dissolved HCl with the remaining HOCl in the solution.

Figure 8 illustrates ClONO₂, HCl, HOCl, and Cl₂ signals as a function of the injector position with a) $P_{\text{HCl}} > P_{\text{ClONO}_2}$ and b) $P_{\text{ClONO}_2} > P_{\text{HCl}}$, conducted at 203 K. In Figure 8(a), γ_2 can be calculated from the decay of the ClONO₂ signal or the growth of Cl₂ as a function of the ClONO₂ injector position, both yielding a reaction probability of about 0.02 (the difference is less than 10%). With $P_{\text{ClONO}_2} > P_{\text{HCl}}$ (Figure 8(b)), the HCl decay was initially very fast as Cl₂ rose rapidly. During the process, little HOCl was released. At larger injector distances, the HCl and Cl₂ signals approached zero and an asymptotic value, respectively. The HOCl signal, on the other hand, rose in accord with the ClONO₂ loss. Clearly, at smaller injector distances, the reaction of ClONO₂ with HCl was dominant. A reaction probability of 0.013 was derived from the initial HCl decay or Cl₂ growth, similar to that in Figure 8(a). When the gaseous HCl concentration diminished at larger distances, the ClONO₂ hydrolysis became apparent, with a reaction probability of 0.0035 (obtained from ClONO₂ decay). This later value is nearly identical to that of ClONO₂ hydrolysis determined above. Hence, with ClONO₂ in excess, both reactions 2 and 3 were observed, with reaction probabilities equal to those measured separately for the ClONO₂ hydrolysis and for the ClONO₂ reaction with HCl.

Some experiments were performed by varying the gaseous HCl concentration at a constant temperature. Figure 9 depicts the measured γ_2 's as a function of HCl partial pressure at 200 K and $P_{\text{ClONO}_2} \approx 8 \times 10^{-8}$ Torr. It is evident that γ_2 varies with the HCl partial pressure: a change of

P_{HCl} from 2×10^{-7} to 2×10^{-6} Torr results in γ_2 values from 0.02 to 0.19. This is primarily due to the increase in HCl dissolved in the film at higher P_{HCl} partial pressures, as governed by Henry's law (which linearly relates the concentration of gaseous HCl to that in the liquid).

Results of γ_2 measurements are shown in Figure 10 as a function of temperature. The open and filled symbols correspond to those determined from ClONO_2 decay and Cl_2 growth, respectively. The top axis labels H_2SO_4 wt % estimated from the H_2O vapor pressures in sulfuric acid solutions.^{18,31} In these experiments, the HCl partial pressures fluctuated only slightly in the range of $(3-4) \times 10^{-7}$ Torr, and the initial partial pressures of HCl were always higher than those of ClONO_2 so that the pseudo first-order assumption applied ($P_{\text{ClONO}_2} = 8 \times 10^{-8}$ to 2×10^{-7} Torr). The parameterized temperature dependence of the γ_2 data is also listed in Table 1 with the experimental conditions. The uncertainty in the γ_2 values is approximately $\pm 30\%$ for $\gamma_2 < 0.1$. For larger γ_2 values (which are more sensitive to the gas-phase diffusion), the uncertainty is as large as a factor of 4. Some scatter in γ_2 is also related to variation in HCl partial pressures during the various experiments; a P_{HCl} variation of $(3-4) \times 10^{-7}$ renders about a 20% difference in γ_2 , according to Figure 9.

In Figure 10, γ_2 approaches 0.3 at 195 K, whereas the value at 212 K is more than two orders of magnitude smaller. This profound temperature dependence appears to be correlated with the amount of dissolved HCl in the film: at a fixed $P_{\text{H}_2\text{O}}$ of 3.8×10^{-4} Torr, HCl volatility in H_2SO_4 increases by about three orders of magnitude over the temperature range from 210 to 195 K.^{37,38} As explained above, this volatility behavior is caused jointly by the changing temperature and changing H_2SO_4 content, when $P_{\text{H}_2\text{O}}$ is held constant.

At present the nature of this reaction mechanism is still unknown. It has been proposed that reaction 2. may occur in two steps, i.e., reaction 1 followed by reaction 3;^{39,40} it is also feasible that reaction 3 may enhance reaction 1 by refreshing the liquid surface with H_2O . Alternatively, this reaction mechanism could simply be ClONO_2 reacting directly with HCl. As demonstrated in Figure 6, no appearance of HOCl was observed in the reaction of ClONO_2 with HCl, and almost all the ClONO_2 loss was accountable due to its reaction with HCl (which can be inferred from the Cl_2 rise). These observations do not enable us to separate the overall reaction into steps even if it were taking place in multiple steps. It is also likely that the measured ClONO_2 uptake in the presence of HCl is due to reactions with both HCl and H_2O . The relative

importance of reactions 1 and 2 is discussed below.

Also, separation of the measured γ_2 as being due to reaction on the surface or in the bulk is not facile. Diffusion of ClONO_2 into the bulk and its subsequent reaction with dissolved HOCl would enhance the uptake taking place at the surface. We did not observe any further changes in the ClONO_2 signal (nor Cl_2) after the initial decline (or rise) upon exposure of ClONO_2 to sulfuric acid (Figure 6), suggesting that either the bulk reaction was too small to compete with that on the surface or ClONO_2 diffusion was very rapid so that only the combined reaction was measured. Realization of these processes, however, could be important in calculating the reaction probabilities based on laboratory measured first-order rate coefficients and volatility constants, as pointed out by Hanson and Ravishankara.²⁹

Reaction of HOCl with HCl

Reaction probability measurements between HOCl and HCl (γ_3) were conducted in the same manner as those for the ClONO_2 reaction with HCl . Figure 11 presents a typical HOCl reactive uptake at 203 K. The partial pressures for HCl and HOCl were 5×10^{-7} and 1×10^{-7} Torr, respectively. The HOCl uptake did not change with exposure time and, thus, there were no saturation effects. This is to be expected if the product Cl_2 desorbs rapidly and the other product H_2O incorporates into sulfuric acid. As stated previously, HOCl also physically dissolves in H_2SO_4 solutions. Since the amount of Cl_2 produced was comparable to the HOCl lost, we conclude that the decline in the HOCl signal is mainly due to the reaction with HCl . These observations also confirm the near unit stoichiometry for this reaction.

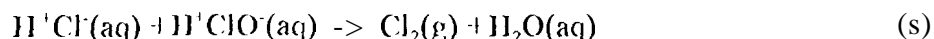
To better quantify the potential effect of 110:1 dissolving in the film on the reaction probability, we determined γ_3 both from the HOCl decay and from the Cl_2 rise. Figure 12 shows signals due to HOCl , HCl , and Cl_2 versus injector position. Two different HOCl partial pressures were employed while the HCl partial pressure was held constant at 5×10^{-7} Torr. In Figure 12(a), the observed first-order loss coefficient for 110 (~1 gave a reaction probability of 0.14 using $P_{\text{HOCl}} = 9 \times 10^{-8}$ Torr. The Cl_2 signal increased with injector distance in accord with the HOCl loss, with a corresponding value of 0.12. Over the length of the substrate, P_{HCl} decreased by about 30%. In Figure 12(b), the HOCl partial pressure (7×10^{-7} Torr) slightly exceeded that of HCl . Again, both

HOCl and HCl were lost as the Cl_2 signal increased. In this case, the decay of HCl followed the first-order rate law, with a γ_3 value of 0.091; the computed reaction probability based on the Cl_2 growth differed by about 15 %.

Results of γ_3 's measured at various HCl partial pressures are plotted in Figure 13. These experiments were performed at 202 K and $P_{\text{HOCl}} \approx 1 \times 10^{-7}$ Torr. The data in this figure display the expected behavior: γ_3 increases with increasing P_{HCl} . An increase in the reaction probability by a factor of 4 is observed as P_{HCl} is varied from 3×10^{-7} to 2×10^{-6} Torr. This is qualitatively the same as that for the ClONO_2 reaction with HCl described above.

The temperature dependence of the HOCl reaction with HCl is illustrated in Figure 14 using HOCl partial pressures of 9×10^{-8} to 1×10^{-7} Torr. The HCl partial pressure was maintained in the range of $(3-4) \times 10^{-7}$ Torr. The symbols are the same as in Figure 9; coefficients of a polynomial fit of the data are summarized in Table 1. The estimated uncertainty for these measurements is similar to that discussed in the proceeding section for the ClONO_2 reaction with HCl.

Reaction probabilities of HOCl with HCl are in general larger than those measured for ClONO_2 reacting with HCl (Figures 10 and 14) by a factor of 3-7. For example, γ_3 is greater than 0.3 at 197 K and decreases to about 0.004 at 215 K. This apparently reflects the higher solubility of HOCl in sulfuric acid: the Henry's law volatility coefficient for HOCl is about an order of magnitude greater than that for HCl under the same conditions.³⁸ The mechanism for the reaction of HOCl with HCl is likely to be acid-based catalysis, occurring after the uptake and subsequent solvation of both species,



Reaction (5) has been investigated by Eigen and Kustin⁴¹ at room temperature. It was found to be limited by liquid-phase diffusion.

The Effect of HNO_3 on Reactions 2 and 3

The effect of HNO_3 on reaction probabilities of HCl with ClONO_2 and HOCl has been examined by first exposing the acid film to HCl and HNO_3 vapors and allowing them to equilibrate with the liquid. Because these experiments dealt virtually with the

HNO₃/HCl/H₂SO₄/H₂O quaternary system, it would be important to verify the reaction products or to look for possible new reactions, if any.

Mass scans before and after exposure of HOCl to sulfuric acid are shown in Figure 15 in the mass range from 30 to 100 amu. For smaller masses less than 30 amu, the presence of He, H₂O, and N₂ (i.e., $m/e = 4, 18, 28$) in high concentrations tended to distort (or saturate) the spectra, because the mass spectrometer was operated at a very high multiplier voltage (i.e. 1.8 KV). At larger masses greater than 100 amu the spectra were featureless. The experiment was conducted at 198 K and partial pressures of 1×10^{-7} , 5×10^{-7} , and 5×10^{-7} Torr for HOCl, HCl, and HNO₃, respectively. The mass spectra of HCl, HNO₃, and HOCl before the exposure show their characteristic peaks at $m/e = 36, 46$ and 52 , with very little impurities (Figure 15(a)). Other mass peaks at $m/e = 32$ and 44 were due to background O₂ and CO₂ and did not interfere with the measurements. After the exposure (Figure 15(b)), several changes are seen in the mass spectra that reveal the reaction mechanism. The appearance of $m/e 70, 72$, and 74 shows the formation of Cl₂, accompanied by the complete disappearance of HOCl. Some loss in gaseous H₂O was also evident due to the reaction with HOCl. The intensity at mass peak $m/e = 46$ (corresponding to HNO₃) remained unchanged during this process. Also, there was no evidence for the occurrence of Cl₂O ($m/e = 86$), which has been suggested to form by the self-reaction of HOCl in sulfuric acid.²⁷ These observations are consistent with the reaction of HOCl with HCl to form Cl₂ in this multi-component system.

Figure 16 represents HOCl, HCl, and Cl₂ signals as a function of injector distance: both experiments were performed under the same conditions except that HNO₃ was present at a partial pressure of $\sim 5 \times 10^{-7}$ Torr in Figure 16(b). As apparent in this Figure, the HOCl decay (or Cl₂ growth) with injector distance did not change noticeably with the addition of HNO₃; the resulting reaction probabilities were within 10%. Note that, although temperature and H₂O partial pressure in Figures 16(a) and (b) were the same, the concentrations of H₂SO₄ in the films were different. This is a result of changing H₂SO₄ content in the H₂SO₄/HNO₃/H₂O ternary system; at a given temperature, addition of HNO₃ to sulfuric acid solutions lowered the H₂O partial pressure so that extra H₂O was needed to hold the H₂O partial pressure constant. A similar phenomenon affects the sulfate aerosol composition in the stratosphere.^{15,16}

Results of reaction probabilities for reaction 3 performed on the H₂SO₄/HNO₃/H₂O/H₂O

quaternary system are displayed in Figure 17 in the temperature range of 198-209 K, along with the measured γ_3 's excluding HNO_3 (the same as the solid line in Figure 14). At 198 K, the liquid film could contain as much as 5 wt % HNO_3 , inferred from the ternary vapor pressure data of Zhang et al.¹⁵ Clearly, the difference in the reaction probabilities was negligible, considering experimental uncertainties and scatter in the present data.

Similarly, we studied reaction probabilities for reaction 2 in this quaternary system. Figure 18 shows mass spectra before and after exposing ClONO_2 to the film. In this case, contributions to mass peaks m/e 46 were due to both ClONO_2 and HNO_3 . As shown in this figure, Cl_2 is produced while gaseous HCl is lost, confirming no additional reactions involved.

Figure 19 shows ClONO_2 , HCl , and Cl_2 signals versus injector position for experiments a) without and b) with HNO_3 . A complication in Figure 19(b) is that ClONO_2 decay can no longer be employed to derive the first-order coefficient because of the interference from HNO_3 . This problem, however, can be remedied by using the Cl_2 growth in both cases. Again, addition of 1 HNO_3 did not appear to influence the Cl_2 growth as a function of the injector distance. Reaction probabilities derived from Figures 19(a) and (b) agreed within 10%.³⁰

The fact that reaction probabilities for reactions 2 and 3 are not significantly affected due to the incorporation of HNO_3 into H_2SO_4 solutions is intriguing. A possible explanation is that both reactions produce Cl_2 , which does not dissolve in sulfuric acid. Furthermore, at a given H_2O partial pressure, the dissolution of HNO_3 in sulfuric acid does not significantly alter the HCl volatility at temperatures near 200 K; instead, it may make HCl slightly more soluble, by reducing the H_2SO_4 content.³⁷

Discussion

Comparison with Previous Results

The ClONO_2 hydrolysis on liquid sulfuric acid has been previously investigated by several groups.^{22,27,29,42} In Figure 20, comparison is made between the present results and previous measurements. The open squares are data measured at 210 K by Tolbert et al.,²⁷ the open triangles are data at 223 K from Williams et al.⁴² Both studies used a Knudsen cell technique.

The solid squares are the most recent measurements from Hanson and Ravishankara²⁹ at 202 K. Shown as the solid line is the fit of the present data, converted to H₂SO₄ wt % based on the temperature and H₂O partial pressure. The reaction probabilities we obtained are in good agreement with those reported by Hanson and Ravishankara, whereas our values are slightly higher (or lower) than those from the SRI group in less (or more) concentrated H₂SO₄ solutions.

Figure 21 compares our results of reaction 2 with the measurements of Hanson and Ravishankara.²⁹ They investigated γ_2 dependence on the HCl partial pressure at 203 K. The data from their measurements, plotted as the solid squares, are taken at $P_{\text{HCl}} \approx 4 \times 10^{-7}$ Torr. Despite some temperature differences with which the two measurements were carried out, the agreement is excellent. Theoretical predictions of uptake coefficients for reaction 2 by Hanson et al.,²⁸ however, yield results considerably smaller than those in Figure 2.1. It is now realized that this is due to improper assumptions concerning the second-order rate coefficients (k^{II}).

Available laboratory data of reaction probabilities for reaction 3 on sulfuric acid are rather limited. Hanson and Ravishankara^{22,38} studied this reaction for a 60 wt % H₂SO₄ solution: a value of $1.6 \times 10^5 \text{ M}^{-1} \text{ s}^{-1}$ for k^{II} was inferred. On the basis of our measured γ_3 's, we estimate this rate coefficient directly using⁴³

$$1/\gamma_3(\text{obs}) = 1/\alpha + [0.4RT/(D_1 k^{\text{I}})]^{1/2} \quad (6)$$

where α is the mass accommodation (assumed unity here), R the gas constant, T the temperature, ω the mean molecular speed, and $k^{\text{I}} = k^{\text{I}}[\text{HCl}]$ is the pseudo-first-order rate coefficient for the reaction of HOCl with HCl in the liquid. Values of liquid-phase diffusion coefficients (D_1) and effective Henry's law coefficients (H^*), needed to extract k^{II} , are taken from the results of Hanson and Ravishankara.³⁸ The calculated k^{II} ranges from 1.35×10^5 to about $1.0 \times 10^4 \text{ M}^{-1} \text{ s}^{-1}$ for acid contents from 60 to 50 wt %: for the 60 wt % H₂SO₄, the value for k^{II} is consistent with that reported by Hanson and Ravishankara.^{22,38} The γ_3 's computed by Hanson et al.,²⁸ assuming a constant k^{II} , exhibit some systematic departure from the present results.

Relative Importance between ClONO₂ Hydrolysis and ClONO₂ Reaction with HCl

As discussed above, in the experiments when HCl is absent, HOCl is the only product of the reaction of ClONO₂ with H₂O (Figure 3). With addition of gaseous HCl at a partial pressure

of $(3-4) \times 10^{-7}$ Torr (which is equivalent to the HCl mixing ratio of a few ppbv in the stratosphere), no HOCl is liberated into the gas phase when HCl is in excess over ClONO₂ (Figure 6). Inspection of Figure 6 may lead, at first sight, to the conclusion that ClONO₂ hydrolysis will be less important because no gaseous HOCl can be produced. This, however, may not be necessarily true for submicron-sized sulfate aerosols in the stratosphere. Consider a spherical droplet of radius a . The characteristic time for liquid diffusion within the particle is given by,⁴⁴

$$t = a^2 / (\pi^2 D_l) \quad (7)$$

This diffusion time needs to be compared with the reaction time of HOCl with dissolved HCl (given by the inverse of the first order loss rate coefficient, $1/k'$) to determine the overall reaction product on the droplet. For a stratospheric aerosol of about $0.1 \mu\text{m}$, the ratio of diffusion to reaction time constants is on the order 10^{-3} to 10^{-2} . Therefore, HOCl generated by the ClONO₂ hydrolysis will likely diffuse out of the droplet before having a chance to react with [H]Cl.

in the case of two reactions (i.e. 1 and 2) competing in the liquid in the present measurements, the overall uptake coefficient shown in Figure 10 may be expressed as,²⁸

$$1/\gamma_2(\text{obs}) = 1/a + \omega/[4H^*RTD_l]^{1/2} (k_{\text{H}_2\text{O}}^1 + k_{\text{HCl}}^1)^{1/2} = 1/[\gamma_1(\text{obs})(1+r)^{1/2}] \quad (8)$$

where r is the ratio of the first-order loss rate coefficients for ClONO₂ reaction with H₂O ($k_{\text{H}_2\text{O}}^1$) and dissolved HCl (k_{HCl}^1). From 195 to 210 K, this ratio varies from 52 to 2.4, derived directly from our measured reaction probabilities of $\gamma_1(\text{obs})$ (Figure 5) and $\gamma_2(\text{obs})$ (Figure 10). These values of r are then used to calculate the fraction of ClONO₂ uptake due to reaction with HCl

$$\gamma_2^{\text{HCl}} = r\gamma_2(\text{obs})/(1+r) \quad (9)$$

and due to reaction with H₂O

$$\gamma_2^{\text{H}_2\text{O}} = \gamma_2(\text{obs})/(1+r) \quad (10)$$

The results are portrayed in Figure 22: the calculated contribution of ClONO₂ hydrolysis to the overall uptake coefficient at temperatures of 200 and 210 K is about 6 and 30%, respectively. Clearly, at lower temperatures and at $P_{\text{HCl}} = (3-4) \times 10^{-7}$ Torr the reaction of ClONO₂ with dissolved HCl is dominant.

Correction for Finite Aerosol Sizes

Since reaction probabilities were measured on bulk liquid H_2SO_4 surfaces in this work, application of the present data to the stratosphere requires correction for the finite dimension of the sulfate aerosols. In general, the reaction probability on small aerosols (γ_c) is related to the laboratory measured (γ_m) value by,^{28,44}

$$1/\gamma_c \approx 1/\alpha + 1/[\gamma_m (\coth q + 1/q)] \quad (11)$$

where q is the diffuso-reactive parameter, defined by $q = a(k^1/D)^{1/2}$ or $q = a/l$ (l is the diffuso-reactive length). We have used the diffuso-reactive length for ClONO_2 in sulfuric acid suggested by Hanson and Ravishankara,²⁹ which is inversely proportional to the square root of water activity. To estimate l for HOCl in sulfuric acid, we calculate the first-order loss coefficient based on the measured reaction probabilities of HOCl with HCl , using equation (6) and $H^*(D)^{1/2}$ measured by Hanson and Ravishankara.³⁸

Shown in Figure 23 are the reaction probabilities relevant to a nominal $0.1 \mu\text{m}$ aerosol particle. Figure 23 indicates that γ_c is much smaller than γ_m for reaction 3, while γ_c is very close to γ_m for reactions 1 and 2. Note that the correction for the aerosol size is dependent on a knowledge of ClONO_2 solubility in sulfuric acid, which is not directly measurable. Also, available information on liquid-phase diffusion coefficients in sulfuric acid is very limited. Hence, the treatment using equation (11) may introduce considerable uncertainty.

Reaction Probabilities on the $\text{H}_2\text{SO}_4/\text{HNO}_3/\text{H}_2\text{O}$ Ternary System

We have shown in this work that uptake coefficients for reactions 2 and 3 do not change appreciably on the $\text{H}_2\text{SO}_4/\text{HNO}_3/\text{H}_2\text{O}$ ternary solution compared to those on the $\text{H}_2\text{SO}_4/\text{H}_2\text{O}$ binary solution at temperatures near or slightly less than 200 K. These measurements, however, are restricted to temperatures above 195 K, because of the freezing of the liquid film, in the stratosphere the composition of sulfate aerosols changes rapidly with decreasing temperature, by absorbing H_2O and HNO_3 ; at very low temperatures ($<192 \text{ K}$) the aerosols could transform essentially into HNO_3 and H_2O binary solutions,^{13,15,16} if crystallization is inhibited. In light of previous laboratory observations that incorporation of HNO_3 in sulfuric acid may increase HCl volatility by reducing the H_2SO_4 content,³⁷ reactions 2 and 3 could be enhanced due to dissolution of HNO_3 . The present results reveal that at temperatures near 195 K these reaction

probabilities are already quite high, approaching, a few tenths. As a result, it is likely that in very cold stratospheric regions the rate-limiting step is gas phase diffusion.

Conclusions

In this work we have investigated heterogeneous reactions 1-3 on liquid sulfuric acid surfaces. Reaction probabilities for these reactions have been measured in the temperature range of 195 to 220 K: by maintaining a constant H_2O partial pressure typical of the lower stratosphere, we are able to simulate the composition representative of stratospheric sulfate aerosols. The data reveal that these reactions depend on temperatures or H_2SO_4 wt O/O. The reaction probability for ClONO_2 hydrolysis approaches 0.01 at temperatures below 200 K, whereas the values for ClONO_2 and HOCl reacting with HCl are on the order of a few tenths at 200 K. The results corroborate earlier studies that heterogeneous reactions involving (ClONO_2 , HCl , and HOCl) could provide important pathways for chlorine activation at high latitudes in winter and early spring.^{13,28}

The relative importance or competition between ClONO_2 hydrolysis (reaction 1) and ClONO_2 reaction with HCl (reaction 2) has also been examined. The data imply that in the presence of gaseous HCl molecules at stratospheric concentrations, the reaction of ClONO_2 with HCl is dominant at low temperatures (< 200 K), but the ClONO_2 hydrolysis becomes important at temperatures above 210 K.

Lastly, at temperatures near 200 K or slightly less than 200 K, reaction probability measurements performed on the $\text{H}_2\text{SO}_4/\text{HNO}_3/\text{H}_2\text{O}$ ternary solutions do not exhibit noticeable deviation from those performed on the $\text{H}_2\text{SO}_4/\text{H}_2\text{O}$ binary system, showing little effect of HNO_3 in sulfate aerosols on the ClONO_2 and HOCl reactions with HCl . Our results suggest that at low temperatures (< 195 K) these reaction probabilities are so large that gas phase diffusion is likely the rate-limiting step in the stratosphere.

Acknowledgements

We thank D.R. Hanson, M.J. Molina, A. Tabazadeh, and D.R. Worsnop for helpful discussions. The research described in this paper was performed at the Jet Propulsion Laboratory, California Institute of Technology, under a contract with the National Aeronautics and Space Administration.

References

- (1) Solomon, S. *Rev. Geophys.* **1988**, 26, 13
- (2) Anderson, J.G.; Brune, W.H.; Joyd, S.A.; Starr, W.,; Roewenstein, M.; Podolske, J.R. *J. Geophys. Res.* **1989**, 94, 11480.
- (3) Anderson, J.G.; Toohey, D.W.; Brune, W.H. *Science* **1991**, 251, 39.
- (4) Brune, W.H.; Anderson, J.G.; Toohey, W.D.; Fahey, D.W.; Kawa, S.R.; Jones, R.L.; McKenna, D.S.; Poole, J.R. *Science* **1991**, 252, 1260.
- (5) Webster, C.R.; May, R.D.; Toohey, D.W.; Avallone, L.M.; Anderson, J.G.; Newman, P.,; Iat, L.; Schoeberl, M.R.; Elkins, J.W.; Chan, K.R. *Science* **1993**, 261, 1130.
- (6) DeMore, W. J.; Sander, S.P.; Golden, D.M.; Molina, M.J.; Hampson, R.F.; Kurylo, M. J.; Howard, C.J.; Ravishankara, A.R. "Chemical kinetics and photochemical data for use in stratospheric modeling"; JPL Publ. 92-20, NASA, 1992.
- (7) Toon, O.B.; Iamill, P.; Turco, R.P.; Pinto, J. *Geophys. Res. Lett.* **1986**, 13, 1284.
- (8) Crutzen, P.J.; Arnold, F. *Nature* **1986**, 324, 651
- (9) Iofmann, D.J.; Solomon, S. *J. Geophys. Res.* **1989**, 94, 5029.
- (10) Brasseur, G.P.; Granier, C.; Walters, S. *Nature* **1990**, 348, 626.
- (11) Rodriguez, J.M.; Ko, M.K.W.; Sze, N. J. *Nature* **1991**, 352, 34
- (12) Steele, I. M.; Hamill, P.; McCormick, M.P.; Swissler, T.J. *J. Atmos. Sci.* **1983**, 40, 2055.
- (13) Molina, M.J.; Zhang, R.; Wooldridge, P.J.; McMahon, J.R.; Kohn, J. E.; Chang, I. Y.; Beyer, K.J.D. *Science* **1993**, 261, 418
- (14) Toon, O.; Browell, E.; Gary, B.; Bait, L.; Newman, P.; Puteschel, R.; Russell, P.; Schoeberl, M.; Toon, G.; Traub, W.; Valero, F.; Selkirk, H.; Jordan, J. *Science* **1993**, 261, 1136
- (15) Zhang, R.; Wooldridge, P.J.; Molina, M.J. *J. Phys. Chem.* **1993**, 97, 854
- (16) Tabazadeh, A.; Turco, R.P.; Jacobson, M.Z. *J. Geophys. Res.* **1994**, 99, 12,897
- (17) Middlebrook, A.M.; Iraci, I.T.; McNeill, I.S.; Koehler, B.G.; Wilson, M.A.; Saastad, O.W.; Tolber, M.A.; Anderson, D.R. *J. Geophys. Res.* **1993**, 98, 20,473.
- (18) Zhang, R.; Wooldridge, P.J.; Abbatt, J.P.D.; Molina, M.J. *J. Phys. Chem.* **1993**, 97, 735
- (19) Zhang, R.; Ieu, M.T.; Keyser, J. Unpublished results.

- (20) Mozurkewich, M.; Calvert, J.G. *J. Geophys. Res.* 1988, 93, 15,889.
- (21) Van Doren, J. M.; Watson, I. R.; Davidovits, P.; Worsnop, D. R.; Zahniser, M.S.; Kolb, C.E. *J. Phys. Chem.* 1991, 95, 1684.
- (22) Hanson, D.R.; Ravishankara, A.R. *J. Geophys. Res.* 1991, 96, 5081.
- (23) Fried, A.; Calvert, J. G.; Mozurkewich, M. *J. Geophys. Res.* 1994, 99, 3517.
- (24) Hanson, D. R.; Ravishankara, A.R. *J. Geophys. Res.* 1993, 98, 22,931.
- (25) Zhang, R.; Jayne, J.-P.; Molina, M.J. *J. Phys. Chem.* 1994, 98, 867.
- (26) Watson, I.R.; Van Doren, J. M.; Davidovits, P.; Worsnop, D.R.; Zahniser, M. S.; Kolb, C.E. *J. Geophys. Res.* 1990, 95, 5631.
- (27) Tolbert, M.A.; Rossi, M. J.; Golden, D.M. *Geophys. Res. Lett.* 1988, 15, 847.
- (28) Hanson, D.R.; Ravishankara, A.R.; Solomon, S. *J. Geophys. Res.* 1994, 99, 3615.
- (29) Hanson, D.R.; Ravishankara, A.R. *J. Phys. Chem.* 1994, 96, 5728.
- (30) Chu, L.T.; Leu, M.-T.; Keyser, L.F. *J. Phys. Chem.* 1993, 97, 7779; *ibid.* 12,798.
- (31) Zeleznik, F.J. *J. Phys. Chem. Ref. Data* 1991, 20, 1157.
- (32) Howard, C. J. *J. Phys. Chem.* 1979, 83, 3.
- (33) Brown, R.L. *J. Res. Natl. Bur. Stand. (D, S.)* 1978, 83, 1.
- (34) Marrero, J. L.; Mason, E.A. *J. Phys. Chem. Ref. Data* 1972, 1, 3.
- (35) Leu, M.-T. *Geophys. Res. Lett.* 1988, 15, 17.
- (36) Jansco, G.; Pupezin, J.; Van Hook, W.A. *J. Phys. Chem.* 1970, 74, 2984.
- (37) Zhang, R. PhD. Dissertation, MIT, 1993.
- (38) Hanson, D. R.; Ravishankara, A.R. *J. Phys. Chem.* 1993, 97, 12,309.
- (39) Abbatt, J. P.D.; Beyer, K.D.; Fucaloro, A.F.; McMahon, J.R.; Wooldridge, P.J.; Zhang, R.; Molina, M.J. *J. Geophys. Res.* 1992, 97, 15,819.
- (40) Abbatt, J.P.D.; Molina, M.J. *J. Phys. Chem.* 1992, 96, 7674.
- (41) Eigen, M.; Kustin, K. *J. Am. Chem. Soc.* 1962, 84, 1355.
- (42) Williams, I.R.; Manion, J. A.; Golden, D.M. *J. Appl. Meteor.* 1994, 33, 785.
- (43) Worsnop, D. R.; Zahniser, M.S.; Kolb, C.E.; Gardner, J. A.; Watson, I.R.; Van Doren, J. M.; Davidovits, P. *J. Phys. Chem.* 1989, 93, 1159.
- (44) Schwartz, S.E. in *Chemistry of Multiphase Atmospheric Systems*; Jaeschke, W., Ed.; NATO ASI Series, Vol. G6; NATO: Brussels, 1986.

Table 1. Summary and Parameterization^a of the Reaction Probability (γ) Measurements

Reaction	Coefficients			Experimental Conditions
	a_1	a_2	a_3	
$\text{ClONO}_2 + \text{H}_2\text{O}$	114,3935	-1.0396	0,00229	$P_{\text{H}_2\text{O}} = 3.8 \times 10^{-4}$ $P_{\text{ClONO}_2} = 8 \times 10^{-8}$ to 2×10^{-7} Torr $T = 195$ to 22.0 K
$\text{ClONO}_2 + \text{HCl}$	75.0581	-0.6158	0.0017	$P_{\text{H}_2\text{O}} = 3.8 \times 10^{-4}$ Torr $P_{\text{ClONO}_2} = 8 \times 10^{-8}$ to 2×10^{-7} Torr $P_{\text{HCl}} = 3 \times 10^{-7}$ to 4×10^{-7} Torr $T = 195$ to 212 K
$\text{HOCl} + \text{HCl}$	-42,5380	0,5238	-0,00157	$P_{\text{H}_2\text{O}} = 3.8 \times 10^{-4}$ Torr $P_{\text{HOCl}} = 9 \times 10^{-8}$ to 1×10^{-7} Torr $P_{\text{HCl}} = 3 \times 10^{-7}$ to 4×10^{-7} Torr $T = 195$ to 212 K

^a

$$\log \gamma = a_1 + a_2 T + a_3 T^2$$

FIGURE CAPTIONS

- Figure 1. Schematic diagram of the flow reactor.
- Figure 2. Physical uptake of HCl, HOCl, and HNO₃ when exposed to a 10-cm length sulfuric acid film at $P_{\text{H}_2\text{O}} = 3.8 \times 10^{-4}$ Torr: (a) for HCl at 202 K and $P_{\text{HCl}} = 5 \times 10^{-7}$ Torr, (b) for HOCl at 204 K and $P_{\text{HOCl}} = 1 \times 10^{-7}$ Torr, and (c) for HNO₃ at 202 K and $P_{\text{HNO}_3} = 5 \times 10^{-7}$ Torr. The injector was moved upstream at 2. rei₀) and, for (a) and (b), returned to its original position at 4 min. The average flow velocity of the carrier gas was 890 cm S-1.
- Figure 3. Temporal profiles of ClONO₂ and HOCl as ClONO₂ was exposed and not exposed to a 10-cm length liquid sulfuric acid film. The HOCl signal exhibited a noticeable delay when the injector was positioned both upstream and downstream, as a result of HOCl being physically dissolved in sulfuric acid. Experimental conditions: $P_{\text{ClONO}_2} = 1 \times 10^{-7}$ Torr, $P_{\text{H}_2\text{O}} = 3.8 \times 10^{-4}$ Torr, $P_{\text{He}} = 0.5$ Torr, flow velocity = 897 cm s⁻¹, and $T = 199$ K.
- Figure 4. ClONO₂ and HOCl as a function of injector position, z. (a) O = ClONO₂ decay; (b) A = HOCl growth, = plot of $S'_{\text{HOCl}}(\infty) - S_{\text{HOCl}}(z)$ where $S_{\text{HOCl}}(\infty)$ is the HOCl signal at larger distance (see text for details). Both ClONO₂ decay and HOCl growth are found to follow first-order kinetics, yielding reaction probabilities of 0.012 and 0.010, respectively. Experimental conditions: $P_{\text{ClONO}_2} = 1.2 \times 10^{-7}$ Torr, $P_{\text{H}_2\text{O}} = 3.8 \times 10^{-4}$ Torr, $P_{\text{He}} = 0.5$ Torr, flow velocity = 921 cm s⁻¹, and $T = 199$ K.
- Figure 5. Reaction probability (γ_1) for ClONO₂ hydrolysis on liquid sulfuric acid films as a function of temperature at $P_{\text{H}_2\text{O}} = 3.8 \times 10^{-4}$ Torr. Open circles are γ_1 's determined from ClONO₂ decay, and solid ones from HOCl growth. The solid curve is a polynomial fit to the experimental data and the coefficients are summarized in Table 1. The top axis corresponds to H₂SO₄ wt % estimated from the temperature and $P_{\text{H}_2\text{O}}$ based 011 vapor pressure data of sulfuric acid solutions.^{18,31} Experimental conditions: $P_{\text{ClONO}_2} = 8 \times 10^{-8}$ to 2×10^{-7} Torr, $P_{\text{He}} = 0.5$ Torr, and flow velocity = 890 to 925 cm s⁻¹.
- Figure 6. Temporal profiles of ClONO₂, HCl, Cl₂ and HOCl as ClONO₂ was exposed and not exposed to a 3-cm length liquid sulfuric acid film. With HCl in excess, little,

if any, HOCl was liberated into the gas phase. Experimental conditions: $P_{\text{ClONO}_2} = 1 \times 10^{-7}$ Torr, $P_{\text{HCl}} = 5 \times 10^{-7}$ Torr, $P_{\text{H}_2\text{O}} = 3.8 \times 10^{-4}$ Torr, $P_{\text{He}} = 0.5$ Torr, flow velocity = 931 cm S⁻¹, and $T = 202$ K.

Figure 7. Temporal profiles of ClONO₂ (solid squares), HCl (solid triangles), Cl₂ (open diamonds), and HOCl (open circles) as ClONO₂ was exposed and not exposed to a 10-cm length liquid sulfuric acid film. With ClONO₂ in excess, the gaseous HCl concentration dropped to near zero upon exposure. Both Cl₂ and HOCl were liberated into the gas phase. Experimental conditions: $P_{\text{ClONO}_2} = 6.5 \times 10^{-7}$ Torr, $P_{\text{HCl}} = 3 \times 10^{-7}$ Torr, $P_{\text{H}_2\text{O}} = 3.8 \times 10^{-4}$ Torr, $P_{\text{He}} = 0.5$ Torr, flow velocity = 890 cm S⁻¹, and $T = 202$ K.

Figure 8. ClONO₂ (open triangles), HCl (solid triangles), Cl₂ (open circles), and HOCl (solid squares) as a function of injector position with (a) $P_{\text{HCl}} > P_{\text{ClONO}_2}$ (i.e., $P_{\text{ClONO}_2} = 1.4 \times 10^{-7}$ Torr and $P_{\text{HCl}} = 5.3 \times 10^{-7}$ Torr), and (b) $P_{\text{ClONO}_2} > P_{\text{HCl}}$ (i.e., $P_{\text{ClONO}_2} = 7.2 \times 10^{-7}$ Torr and $P_{\text{HCl}} = 3.3 \times 10^{-7}$ Torr). In (a) the reaction probabilities corresponding to ClONO₂ decay and Cl₂ growth are 0.022 and 0.020, respectively. In (b) the initial HCl decay at smaller injector distances leads to a reaction probability of 0.013, while the ClONO₂ decay at larger injector distances corresponds to a value of 0.0035. Experimental conditions: $P_{\text{H}_2\text{O}} = 3.8 \times 10^{-4}$ Torr, $P_{\text{He}} = 0.5$ Torr, flow velocity = 901 cm s⁻¹, and $T = 203$ K.

Figure 9. Reaction probabilities (γ_2) of ClONO₂ with HCl on liquid sulfuric acid films as a function of P_{HCl} . The solid curve is a polynomial fit to the experimental data. Experimental conditions: $P_{\text{ClONO}_2} \approx 8 \times 10^{-8}$ Torr, $P_{\text{H}_2\text{O}} = 3.8 \times 10^{-4}$ Torr, $P_{\text{He}} = 0.5$ Torr, flow velocity = 900 to 920 cm s⁻¹, and $T = 200$ K.

Figure 10. Reaction probability (γ_2) of ClONO₂ with HCl on liquid sulfuric acid films as a function of temperature at $P_{\text{H}_2\text{O}} = 3.8 \times 10^{-4}$ Torr. The open and filled symbols are γ_2 's determined from ClONO₂ decay and Cl₂ growth, respectively. The solid curve is a polynomial fit to the experimental data and the coefficients are summarized in Table 1. Experimental conditions: $P_{\text{ClONO}_2} = 8 \times 10^{-8}$ to 2×10^{-7} Torr, $P_{\text{HCl}} = 3 \times 10^{-7}$ to 4×10^{-7} Torr, $P_{\text{He}} = 0.5$ Torr, and flow velocity = 890 to 925 cm s⁻¹.

Figure 11. Temporal profiles of HCl, Cl₂ and HOCl as HOCl was exposed and not exposed to a 2-cm length liquid sulfuric acid film. Experimental conditions: $P_{\text{HOCl}} = 1 \times 10^{-7}$

‘1’err, $P_{\text{HCl}} = 5 \times 10^{-7}$ Torr, $P_{\text{H}_2\text{O}} = 3.8 \times 10^{-4}$ ‘1’err, $P_{\text{He}} = 0.5$ ‘1’err, flow velocity = 915 cm s⁻¹, and $T = 203$ K.

Figure 12. HOCl (open squares), Cl₂ (open circles), and HCl (solid triangles) as a function of injector position with (a) $P_{\text{HCl}} > P_{\text{HOCl}}$ ($P_{\text{HOCl}} = 9 \times 10^{-8}$ ‘1’err), and (b) $P_{\text{HOCl}} > P_{\text{HCl}}$ ($P_{\text{HOCl}} = 7 \times 10^{-7}$ ‘1’err). in (a) the reaction probabilities are 0.14 and 0.12 corresponding to HOCl decay and Cl₂ growth, while in (b) these values are 0.091 and 0.10. Experimental conditions: $P_{\text{HCl}} = 5 \times 10^{-7}$ ‘1’err, $P_{\text{H}_2\text{O}} = 3.8 \times 10^{-4}$ ‘1’err, $P_{\text{He}} = 0.5$ ‘1’err, flow velocity = 901 cm s⁻¹, and $T = 198$ K.

Figure 13. Reaction probabilities (γ_3) of HOCl with HCl on liquid sulfuric acid films as a function of P_{HCl} . The solid curve is a polynomial fit to the experimental data. Experimental conditions: $P_{\text{HOCl}} = 1 \times 10^{-7}$ ‘1’err, $P_{\text{H}_2\text{O}} = 3.8 \times 10^{-4}$ ‘1’err, $P_{\text{He}} = 0.5$ ‘1’err, flow velocity = 890 to 925 cm s⁻¹, and $T = 202$ K.

Figure 14. Reaction probability (γ_3) of HOCl with HCl on liquid sulfuric acid films as a function of temperature at $P_{\text{H}_2\text{O}} = 3.8 \times 10^{-4}$ Torr. The open anti filled symbols are γ_3 's determined from the HOCl decay and Cl₂ growth, respectively. The solid curve is a polynomial fit to the experimental data and the coefficients are summarized in Table 1. Experimental conditions: $P_{\text{HOCl}} = 9 \times 10^{-8}$ to 1×10^{-7} ‘1’err, $P_{\text{HCl}} = 3 \times 10^{-7}$ to 4×10^{-7} ‘1’err, $P_{\text{He}} = 0.5$ ‘1’err, and flow velocity = 890 to 925 cm s⁻¹,

Figure 15. Mass spectrometer scans before (a) and after (b) exposure of HOCl to a liquid sulfuric acid film doped with HCl and HNO₃. Experimental conditions: $P_{\text{HOCl}} = 1 \times 10^{-7}$ Torr, $P_{\text{HCl}} = 5 \times 10^{-7}$ ‘1’err, $P_{\text{HNO}_3} = 5 \times 10^{-7}$ ‘1’err, $P_{\text{H}_2\text{O}} = 3.8 \times 10^{-4}$ Torr, $P_{\text{He}} = 0.5$ ‘1’err, flow velocity = 921 cm s⁻¹, and $T = 198$ K. See text for details.

Figure 16. HOCl (open squares), Cl₂ (open circles), and HCl (solid triangles) as a function of injector position without (a) and with (b) HNO₃. Both HOCl decay and Cl₂ growth with injector distance did not change appreciably with addition of HNO₃. Figure 16(a) is the same as Figure 12(a). In (b) the reaction probabilities are 0.135 and 0.140 corresponding to HOCl decay and Cl₂ growth. Experimental conditions: $P_{\text{HOCl}} = 1 \times 10^{-7}$ ‘1’err, $P_{\text{HCl}} = 5 \times 10^{-7}$ Torr, $P_{\text{HNO}_3} = 5 \times 10^{-7}$ ‘1’err, $P_{\text{H}_2\text{O}} = 3.8 \times 10^{-4}$ ‘1’err, $P_{\text{He}} = 0.5$ ‘1’err, flow velocity = 901 cm s⁻¹, and $T = 198$ K.

Figure 17. Reaction probability (γ_3) of HOCl with HCl on liquid sulfuric acid films doped

with HNO_3 , as a function of temperature at $P_{\text{H}_2\text{O}} = 3.8 \times 10^{-4}$ Torr. The solid curve is γ_3 determined earlier without HNO_3 . Experimental conditions: $P_{\text{HOCl}} = 9 \times 10^{-8}$ to 1×10^{-7} Torr, $P_{\text{HCl}} = 3 \times 10^{-7}$ to 4×10^{-7} Torr, $P_{\text{He}} = 0.5$ Torr, and flow velocity = 890 to 925 cm s⁻¹.

Figure 18. Mass spectrometer scans before (a) and after (b) exposure of ClONO_2 to a liquid sulfuric acid film doped with HCl and HNO_3 . Experimental conditions: $P_{\text{ClONO}_2} = 1.4 \times 10^{-7}$ Torr, $P_{\text{HCl}} = 5 \times 10^{-7}$ Torr, $P_{\text{HNO}_3} = 5 \times 10^{-7}$ Torr, $P_{\text{H}_2\text{O}} = 3.8 \times 10^{-4}$ Torr, $P_{\text{He}} = 0.5$ Torr, flow velocity = 921 cm s⁻¹, and $T = 198$ K.

Figure 19. ClONO_2 (open squares), Cl_2 (open circles), anti HCl (solid triangles) as a function of injector position without (a) and with (b) HNO_3 . The Cl_2 growth with injector distance did not change appreciably with addition of HNO_3 . In (a) the reaction probabilities are 0.042 and 0.045 corresponding to ClONO_2 decay and Cl_2 growth, while in (b) the value is 0.046 for Cl_2 growth. Experimental conditions: $P_{\text{ClONO}_2} = 1 \times 10^{-7}$ Torr, $P_{\text{HCl}} = 4 \times 10^{-7}$ Torr, $P_{\text{HNO}_3} = 5 \times 10^{-7}$ Torr, $P_{\text{H}_2\text{O}} = 3.8 \times 10^{-4}$ Torr, $P_{\text{He}} = 0.5$ Torr, flow velocity = 911 cm s⁻¹, and $T = 200$ K.

Figure 20. comparison of reaction probabilities for ClONO_2 hydrolysis among various studies: Hanson and Ravishankara²⁹ (■), Williams et al.⁴¹ (A), and Tolbert et al.²⁷ (□). The solid line represents a fit of the present data.

Figure 21. Comparison of reaction probabilities for ClONO_2 with HCl between this work (solid line) and those reported by Hanson and Ravishankara²⁹ (solid squares).

Figure 22. Partitioning of the overall uptake coefficients of ClONO_2 with dissolved HCl (solid curve) into those due to ClONO_2 hydrolysis (short dashed curve) and due to ClONO_2 reaction with HCl (long dashed curve), using equations (8) to (10). See text for details.

Figure 23. Corrected reaction probabilities (clashed curves) relevant to a nominal 0.1 μm aerosol particle based on equation (11), along with those pertinent to the bulk solutions (solid curves). See text for details.

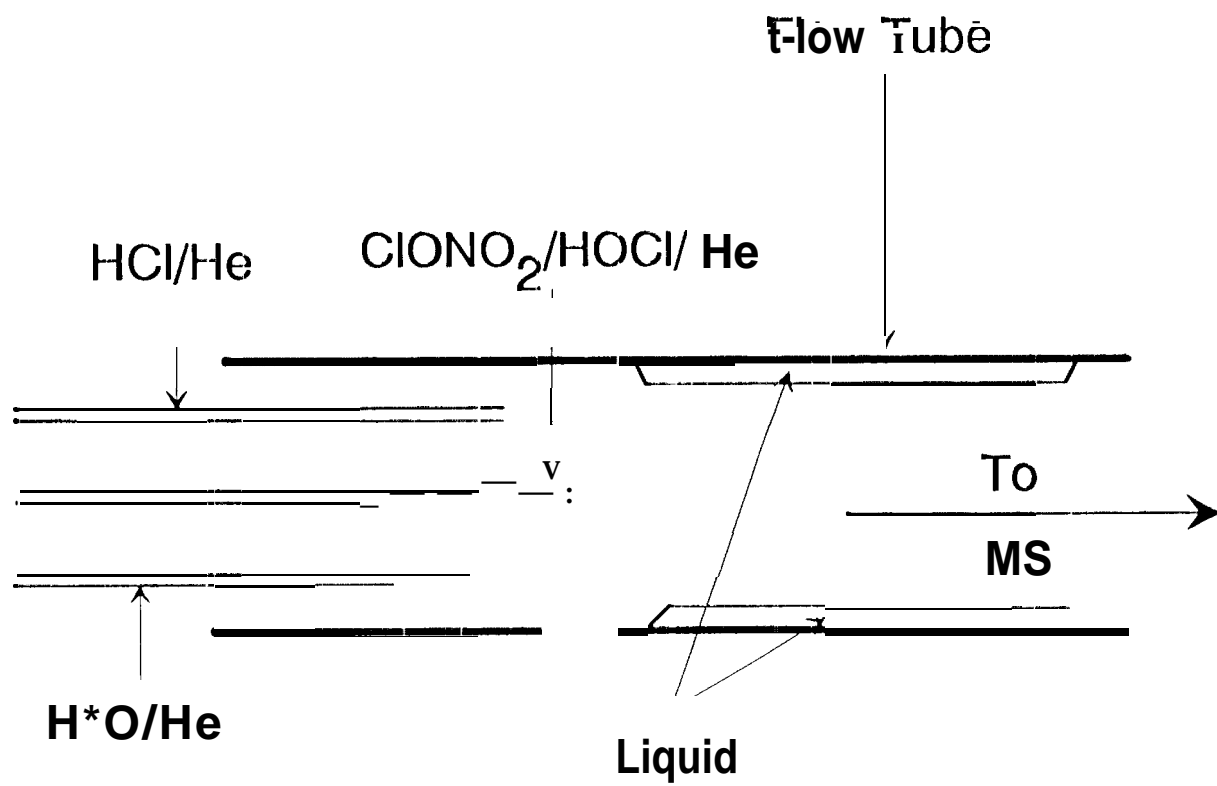


Fig. 1

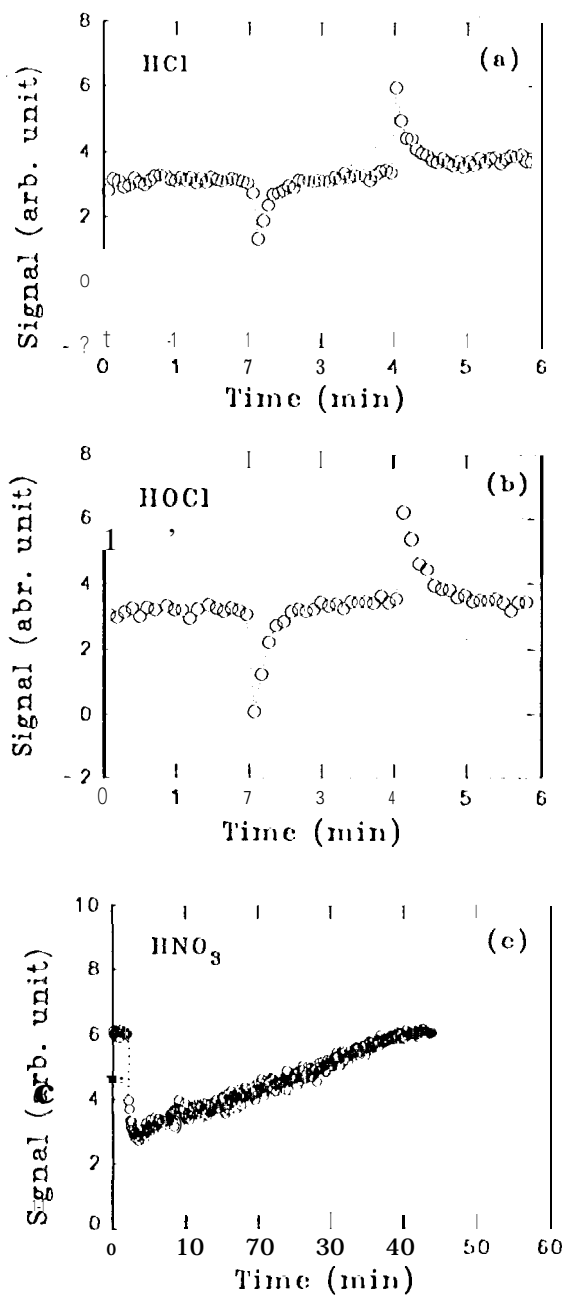


Fig. 2

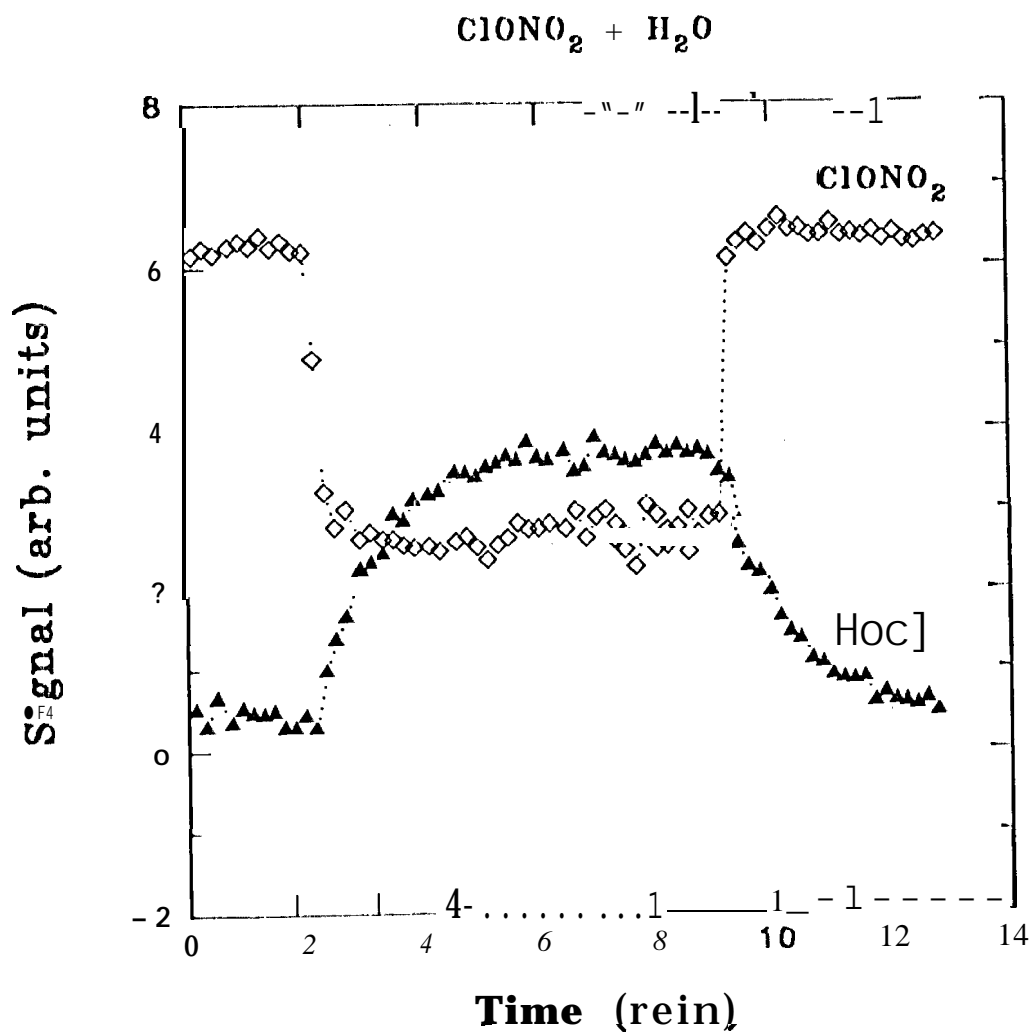


Fig 3

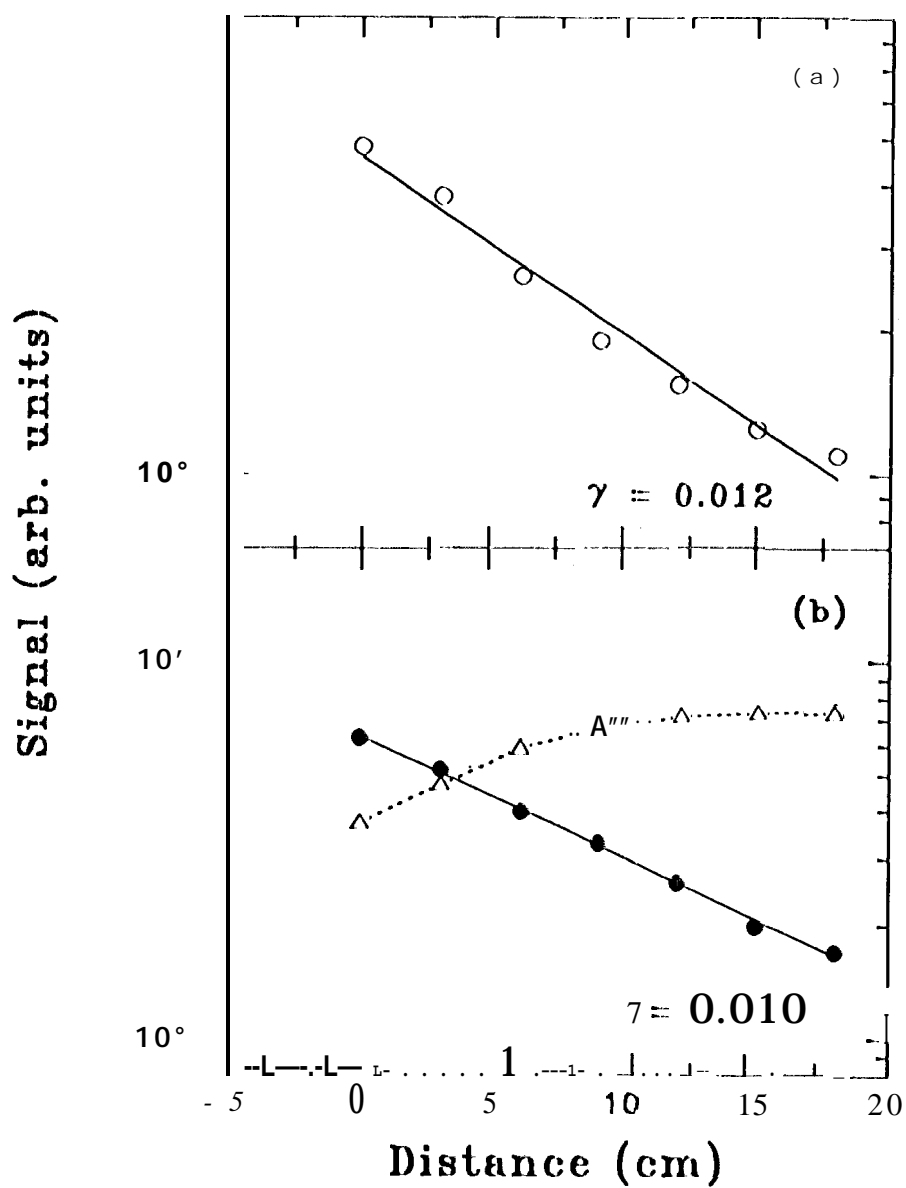
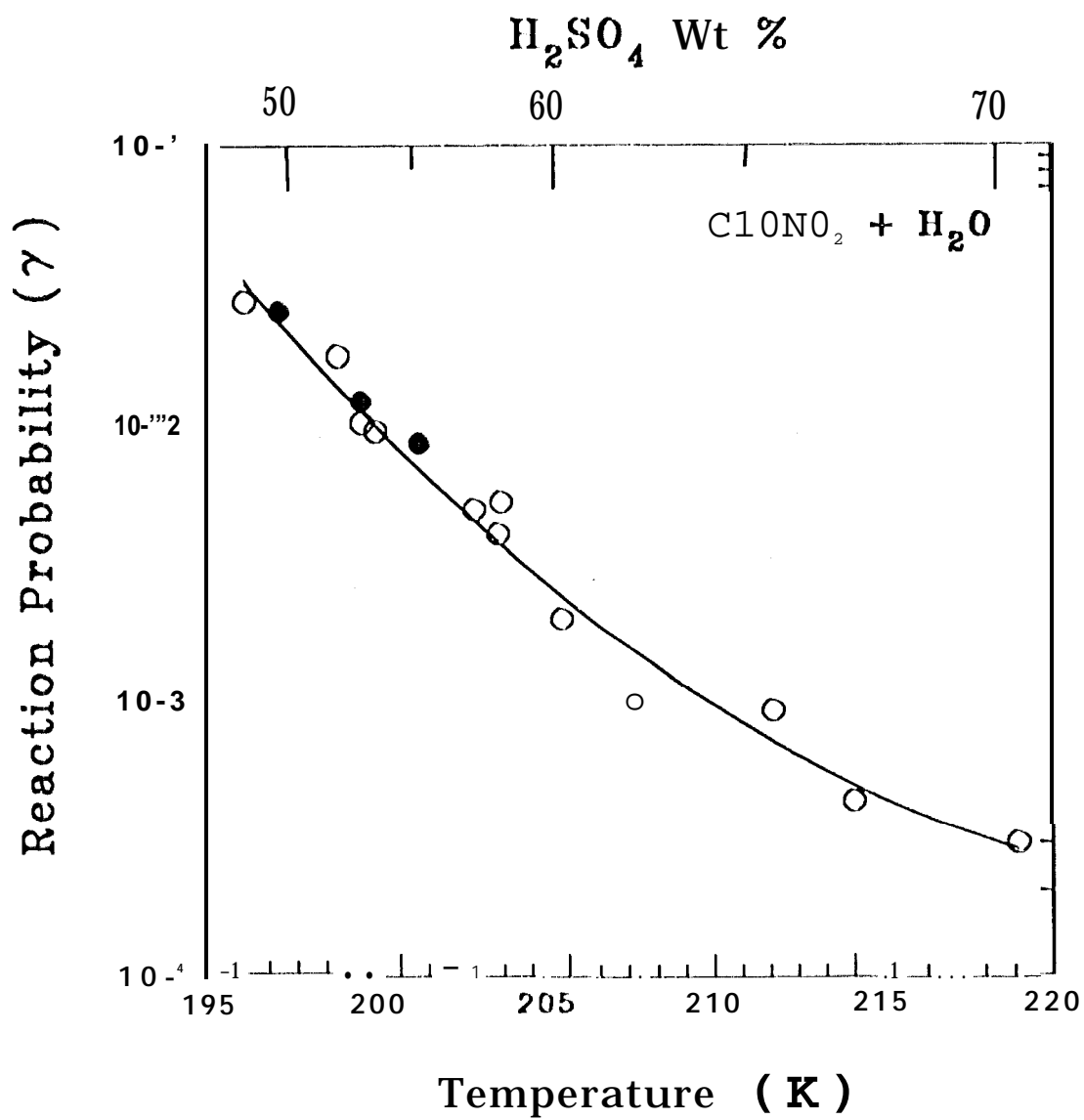


Fig. 4



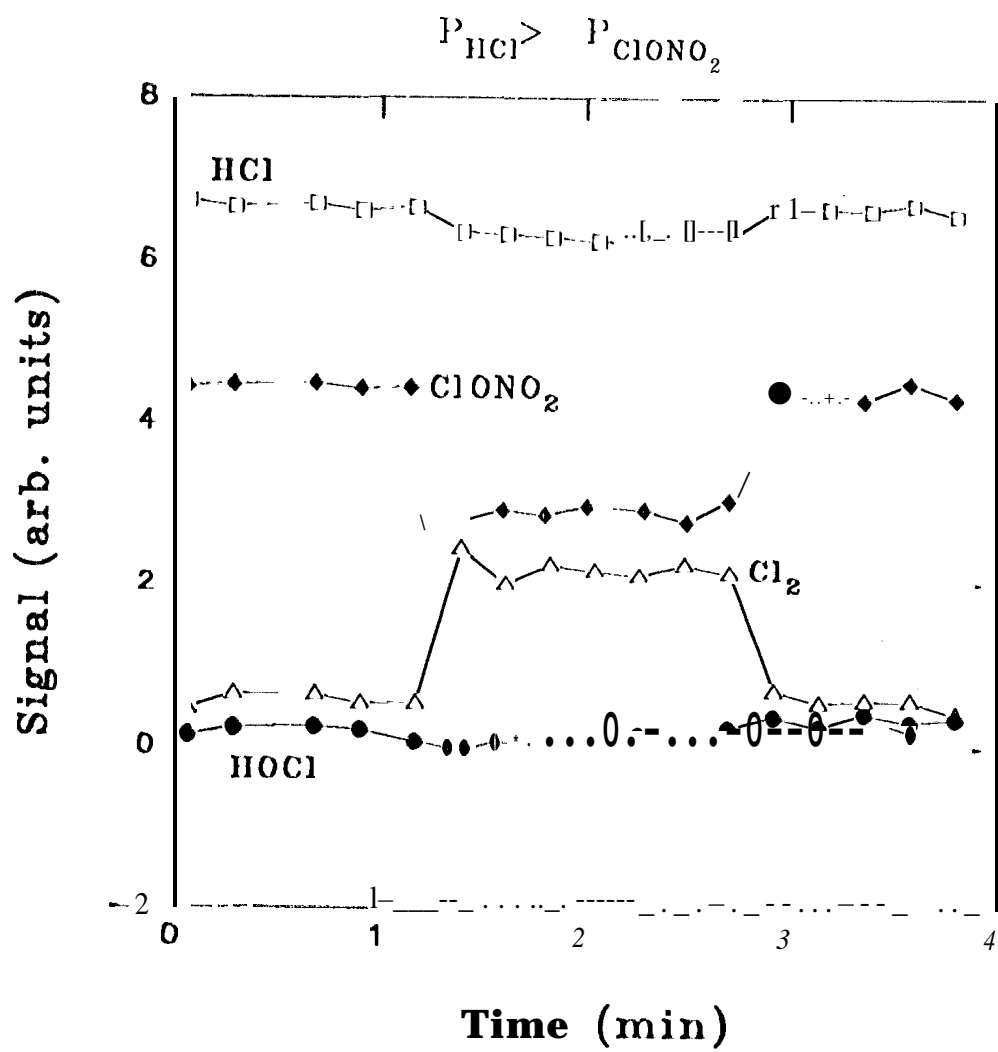
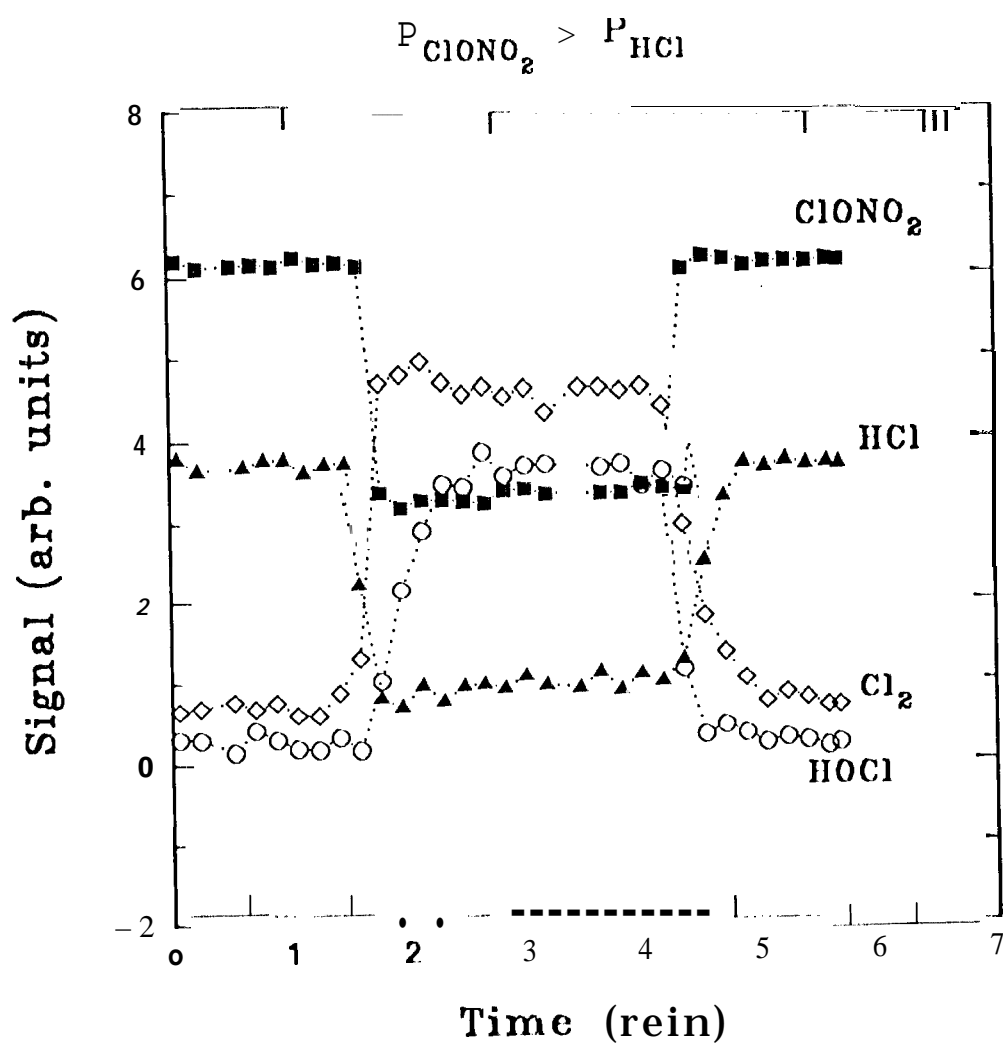


Fig 6



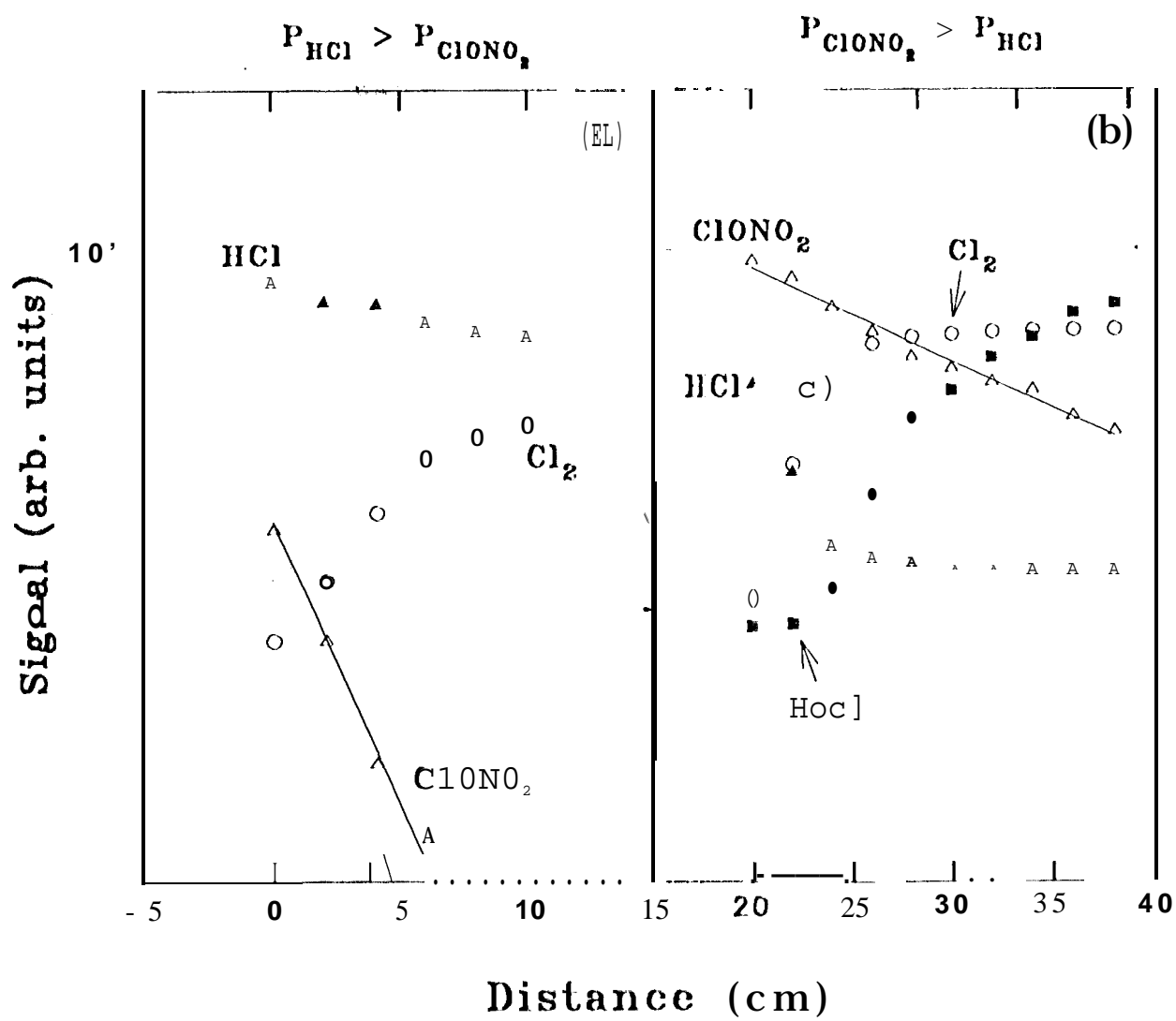


Fig. 8

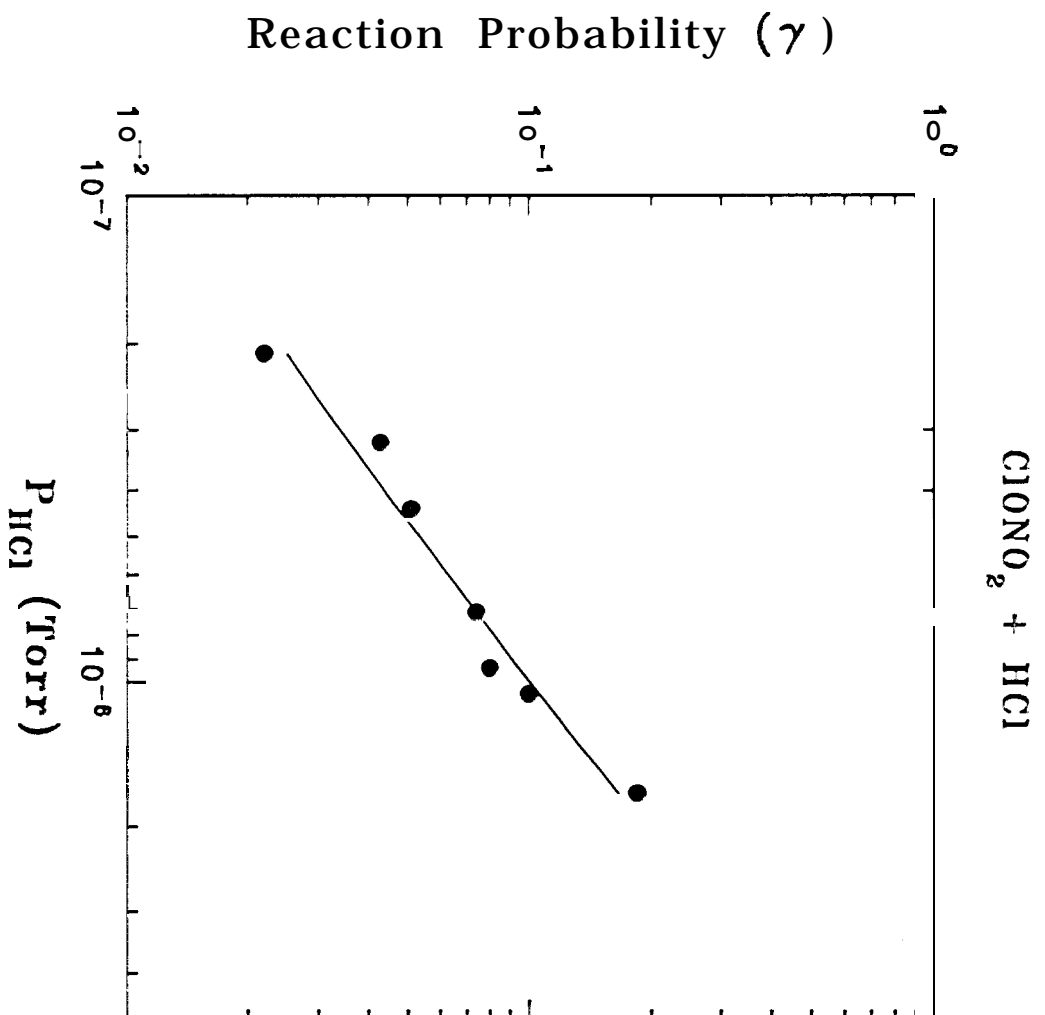
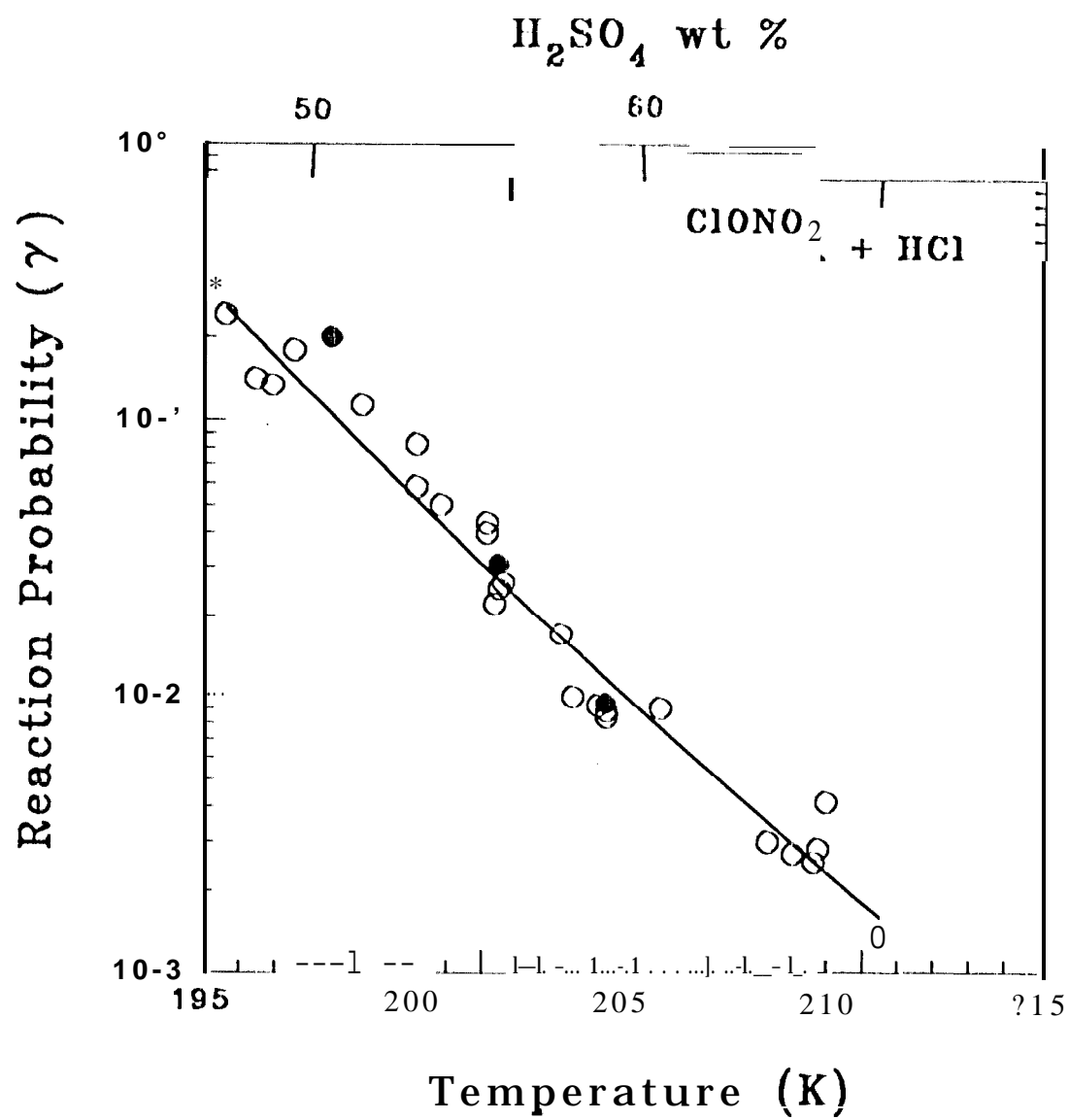


Fig. 9



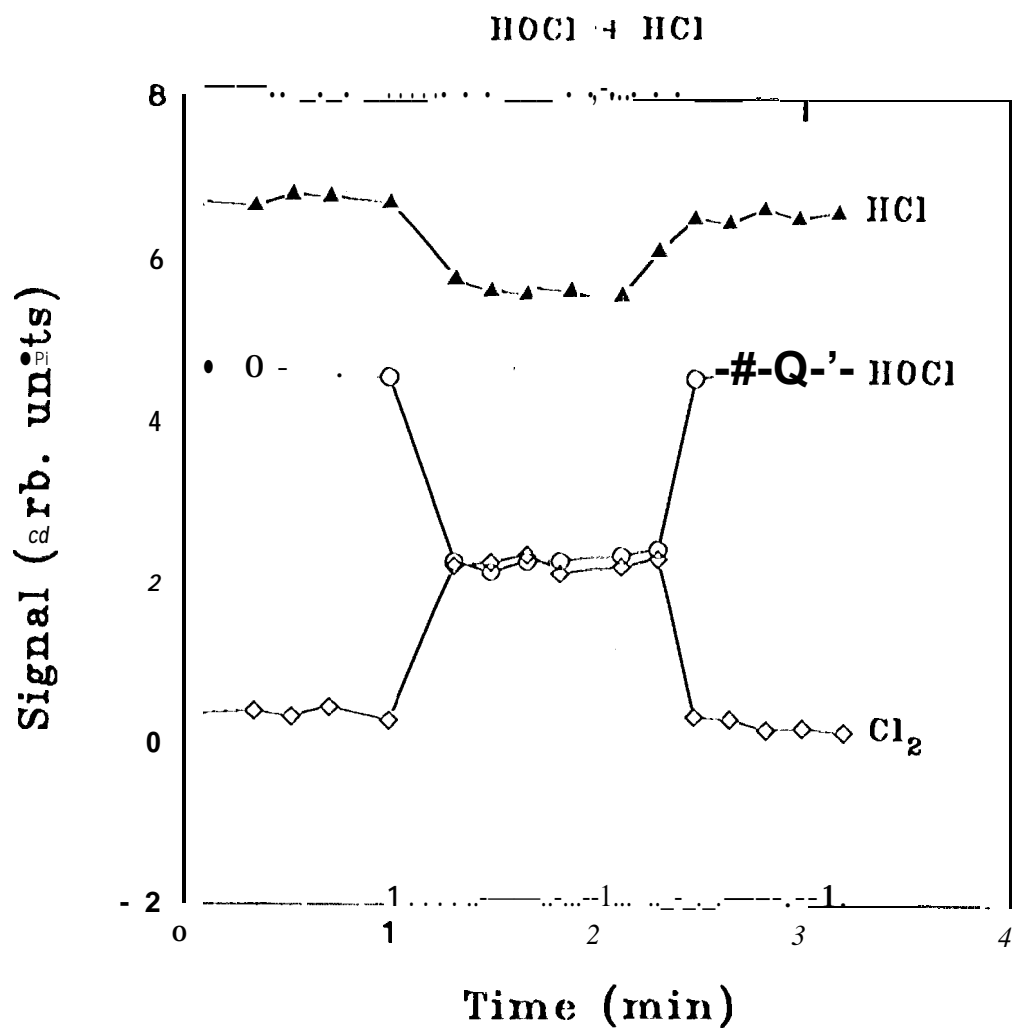
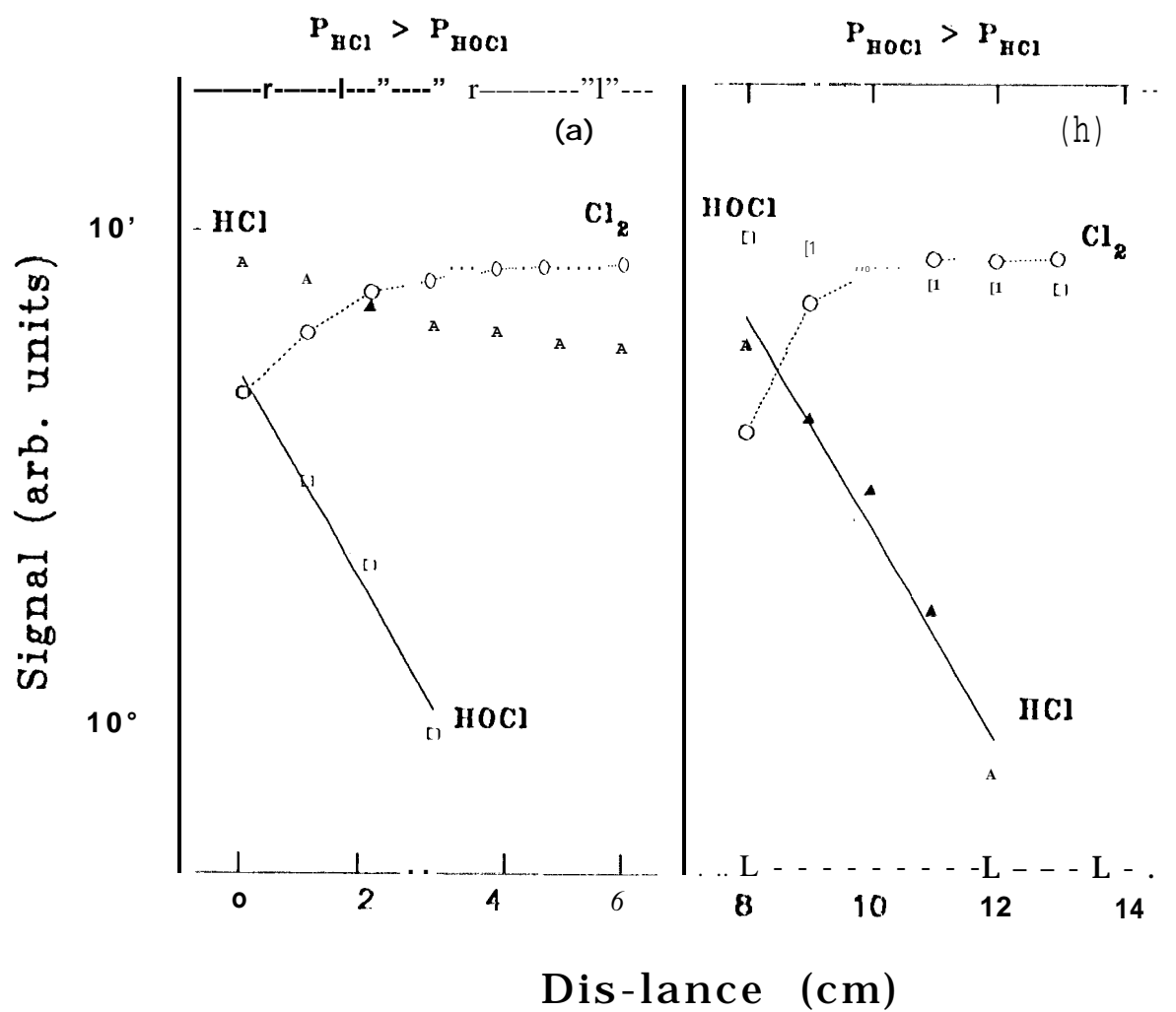
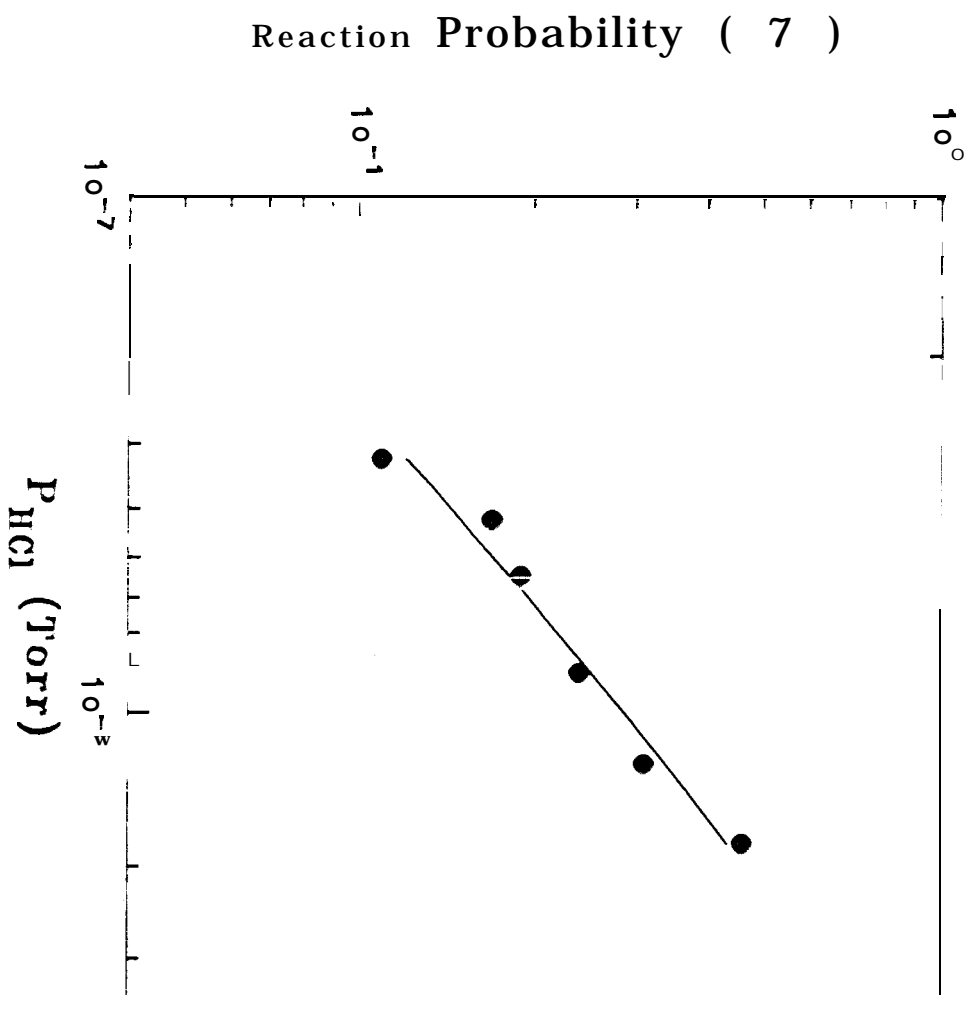
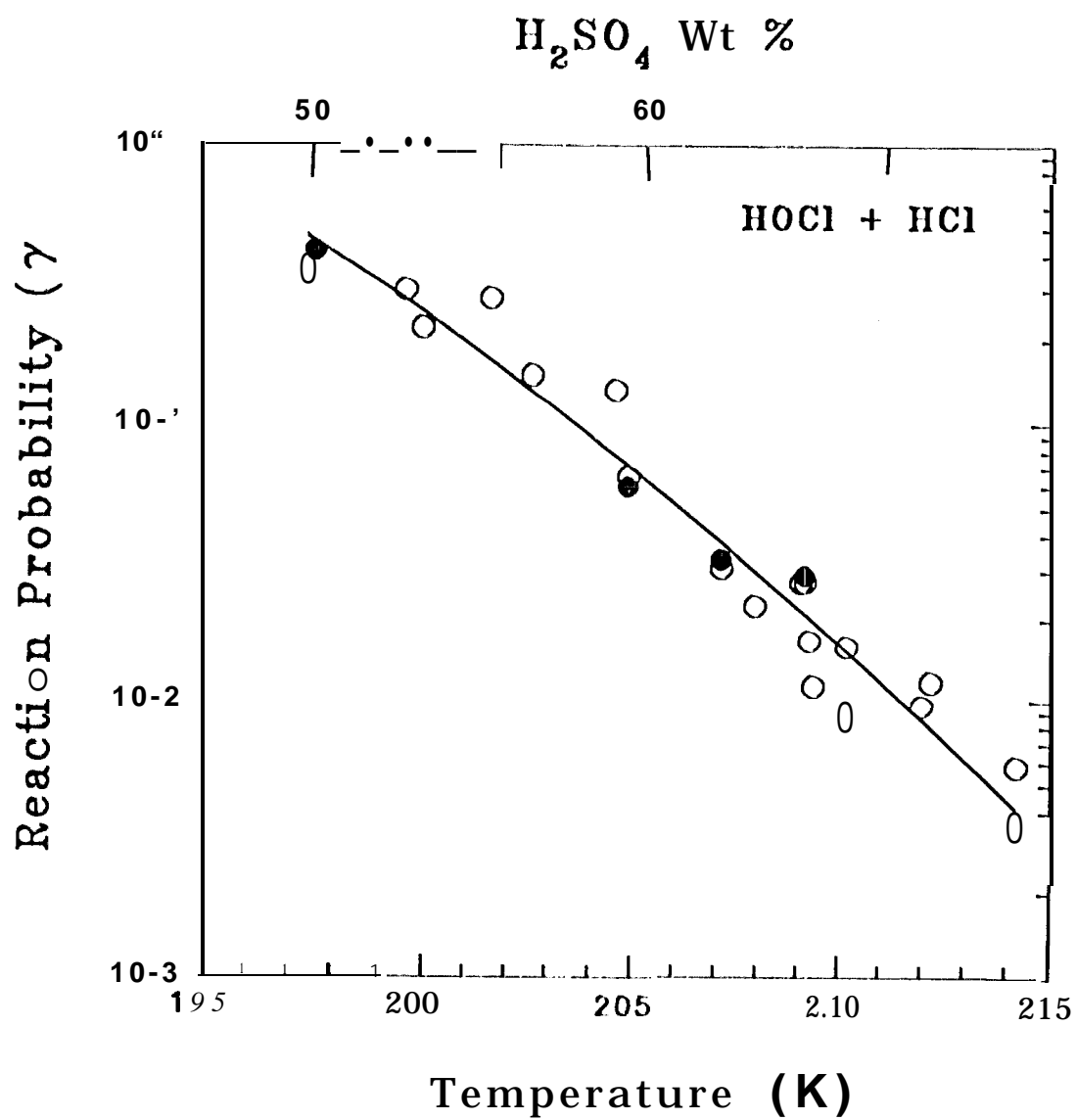


Fig. 11



Figure





HOCl -I- HCl

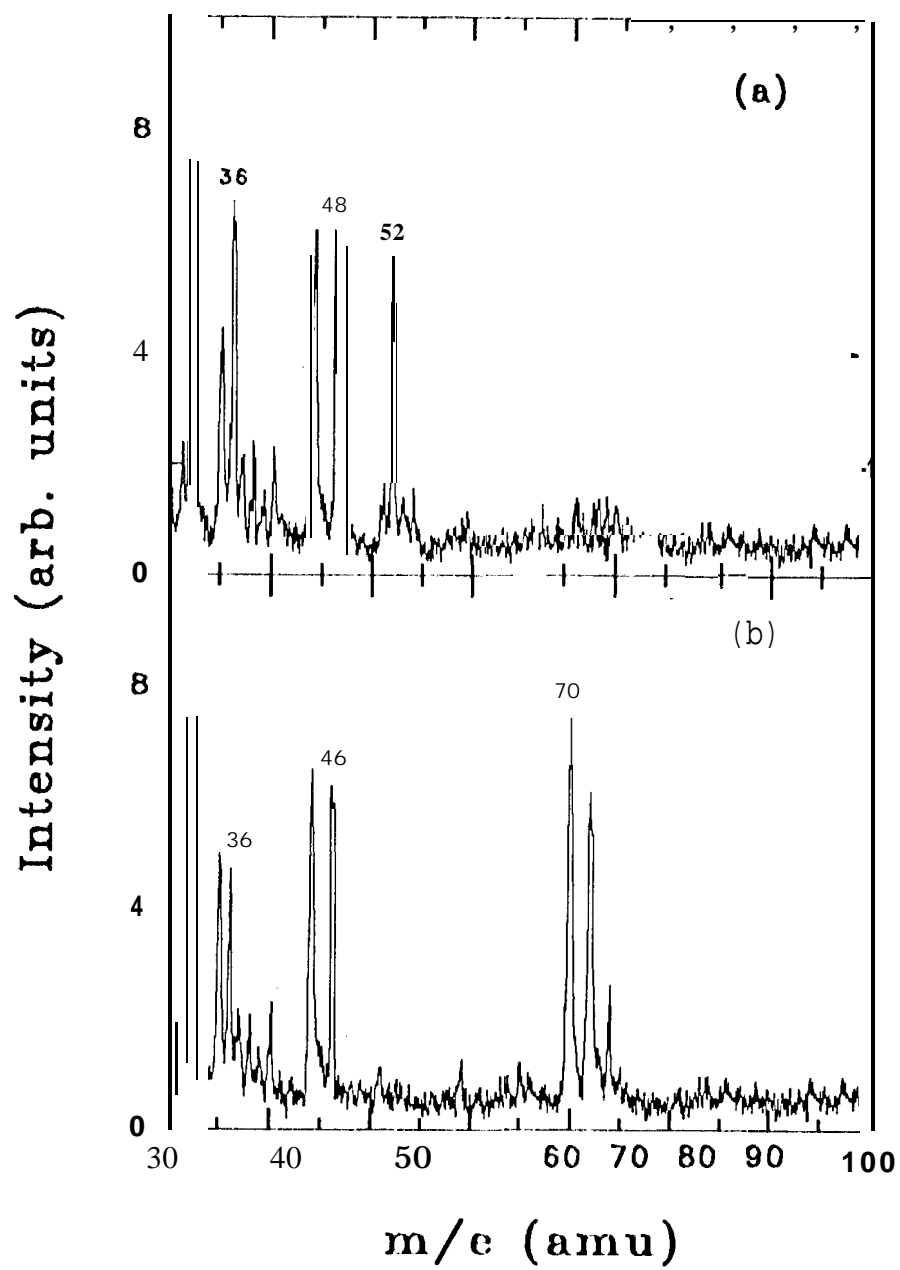


Fig. 15

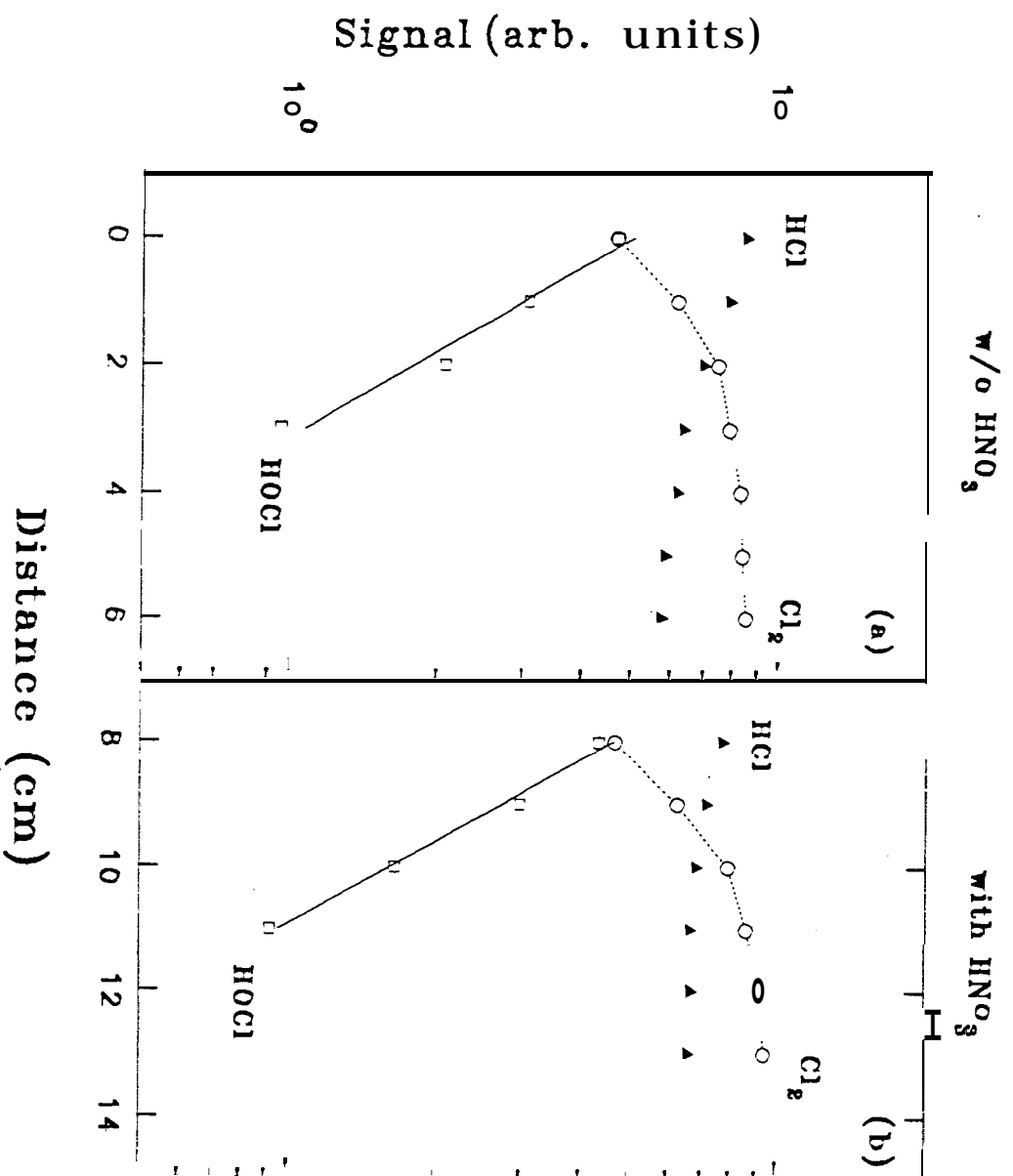


Fig. 9.16

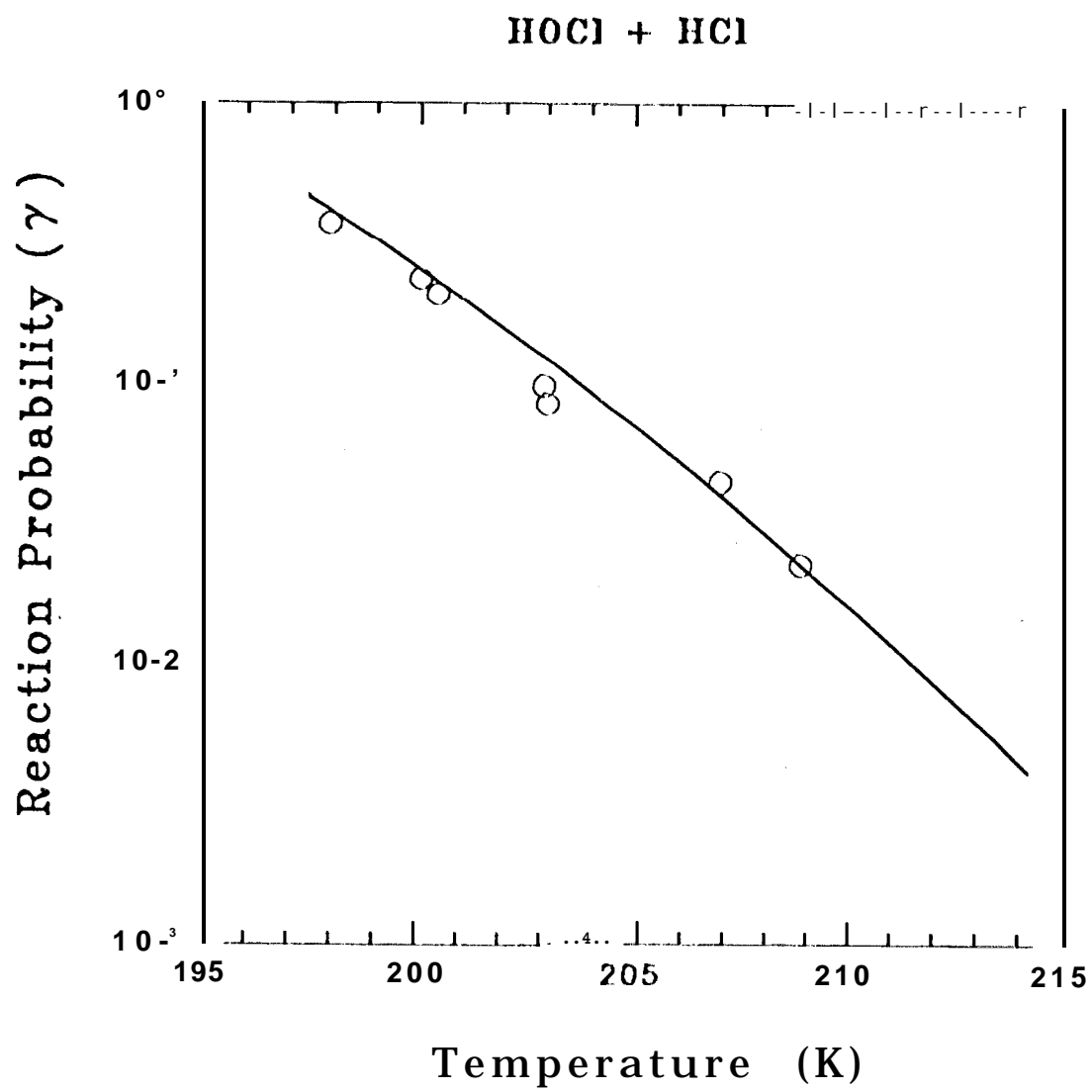


Fig. 17

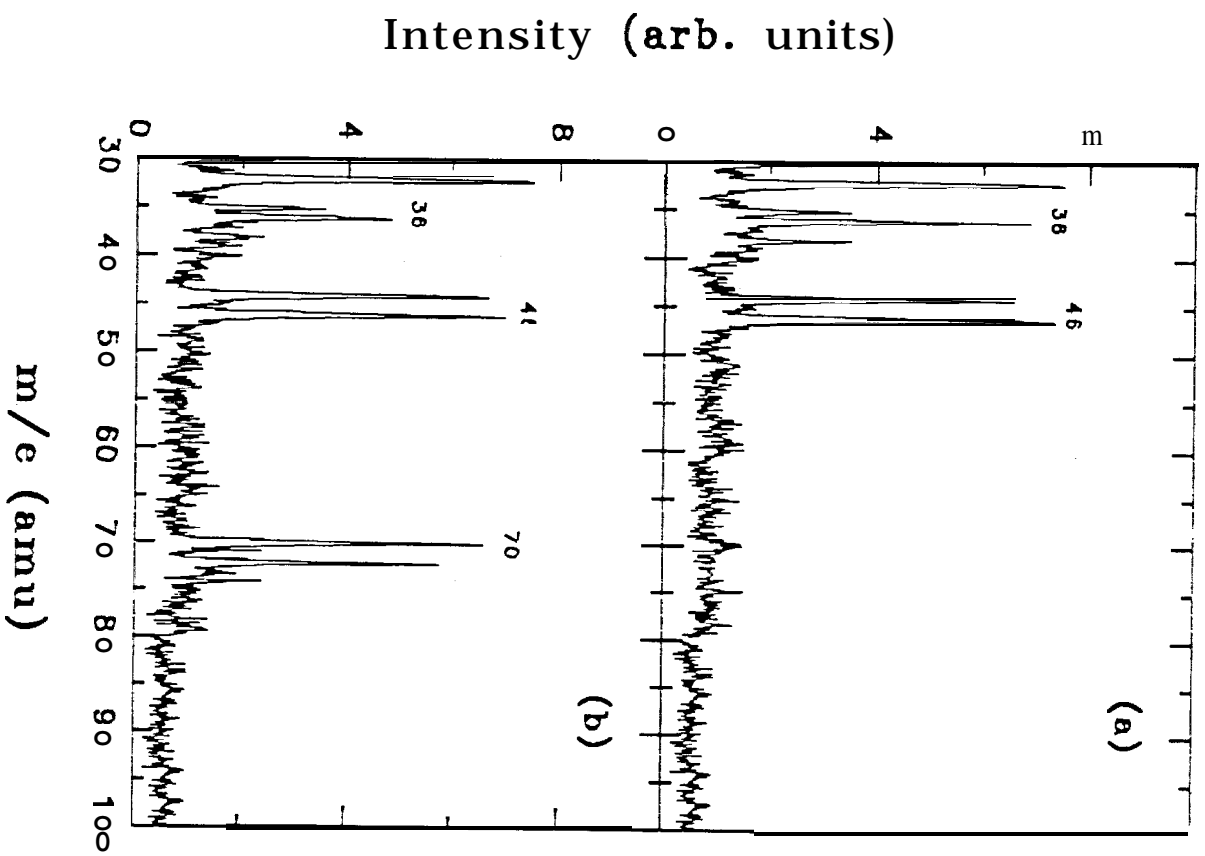
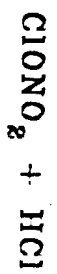


Fig. 18

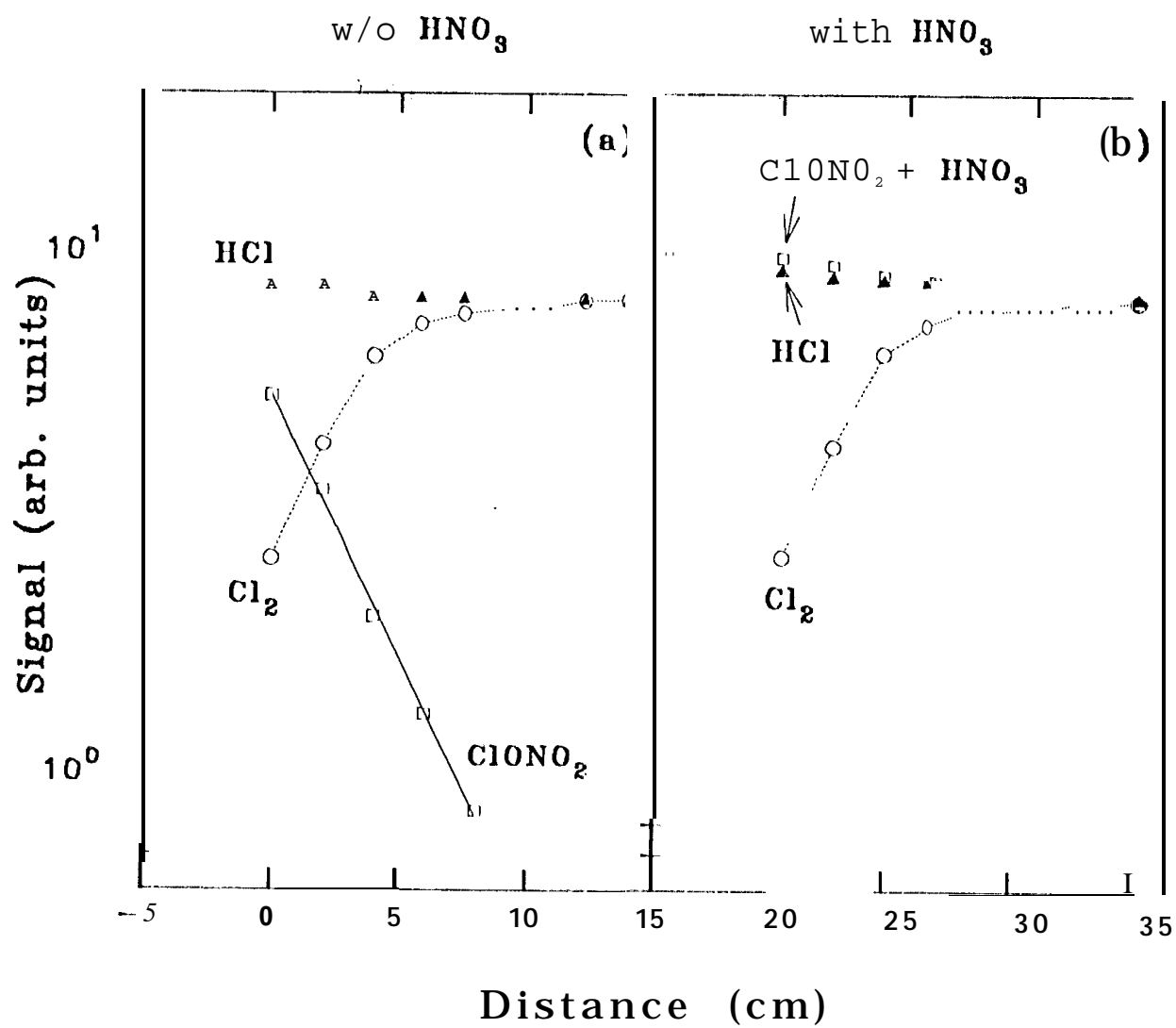


Fig. 19

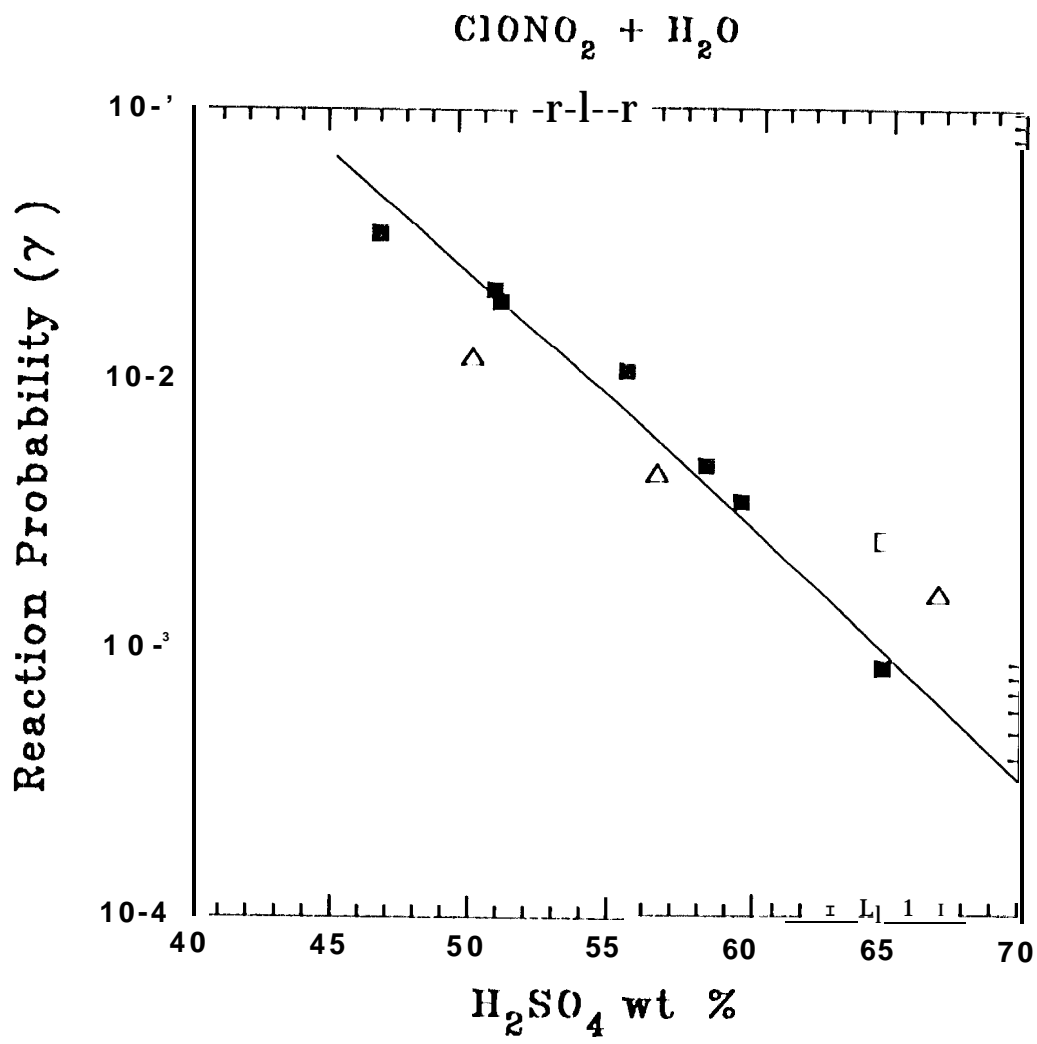


Fig. 20

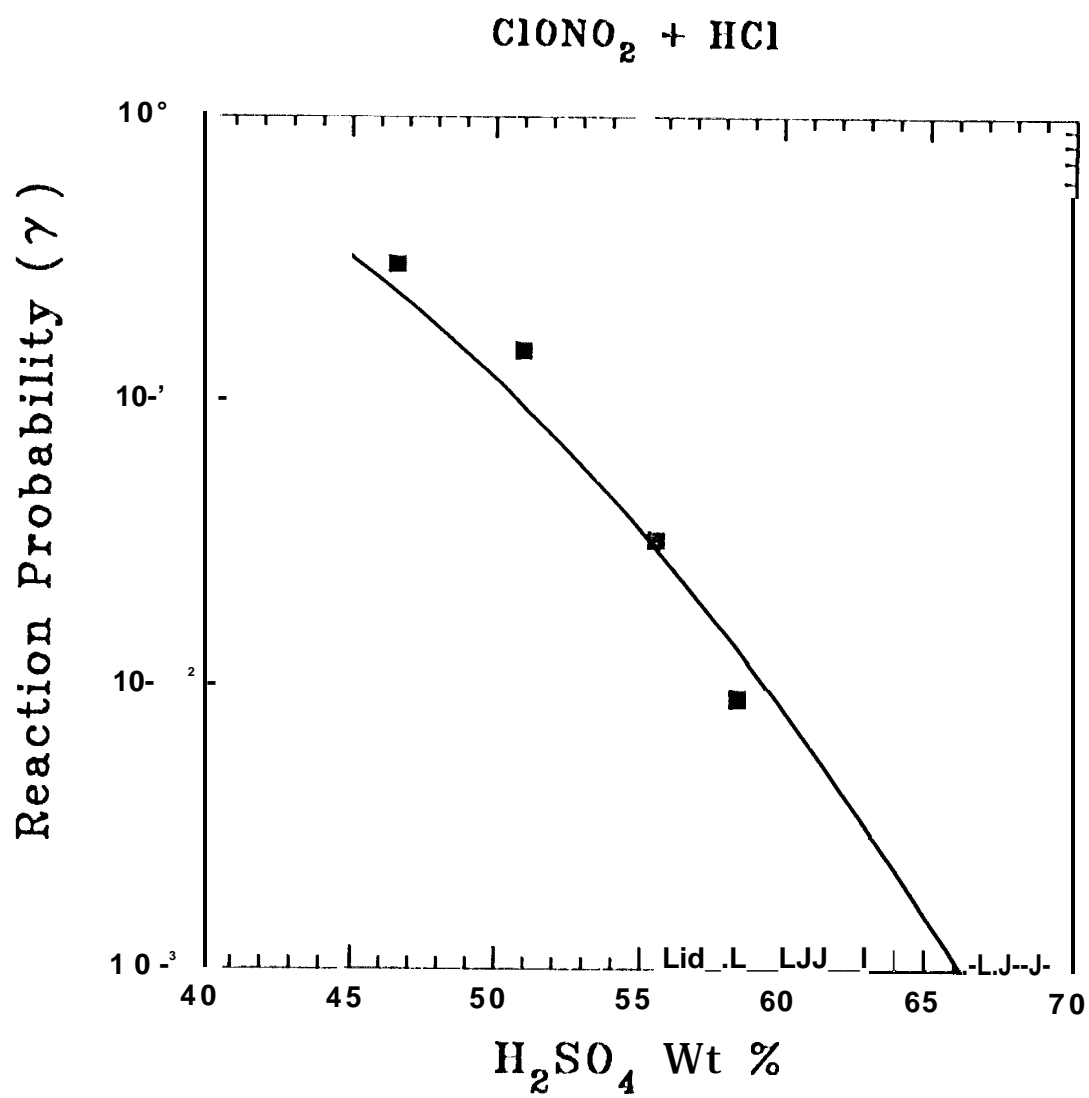


Fig. 21

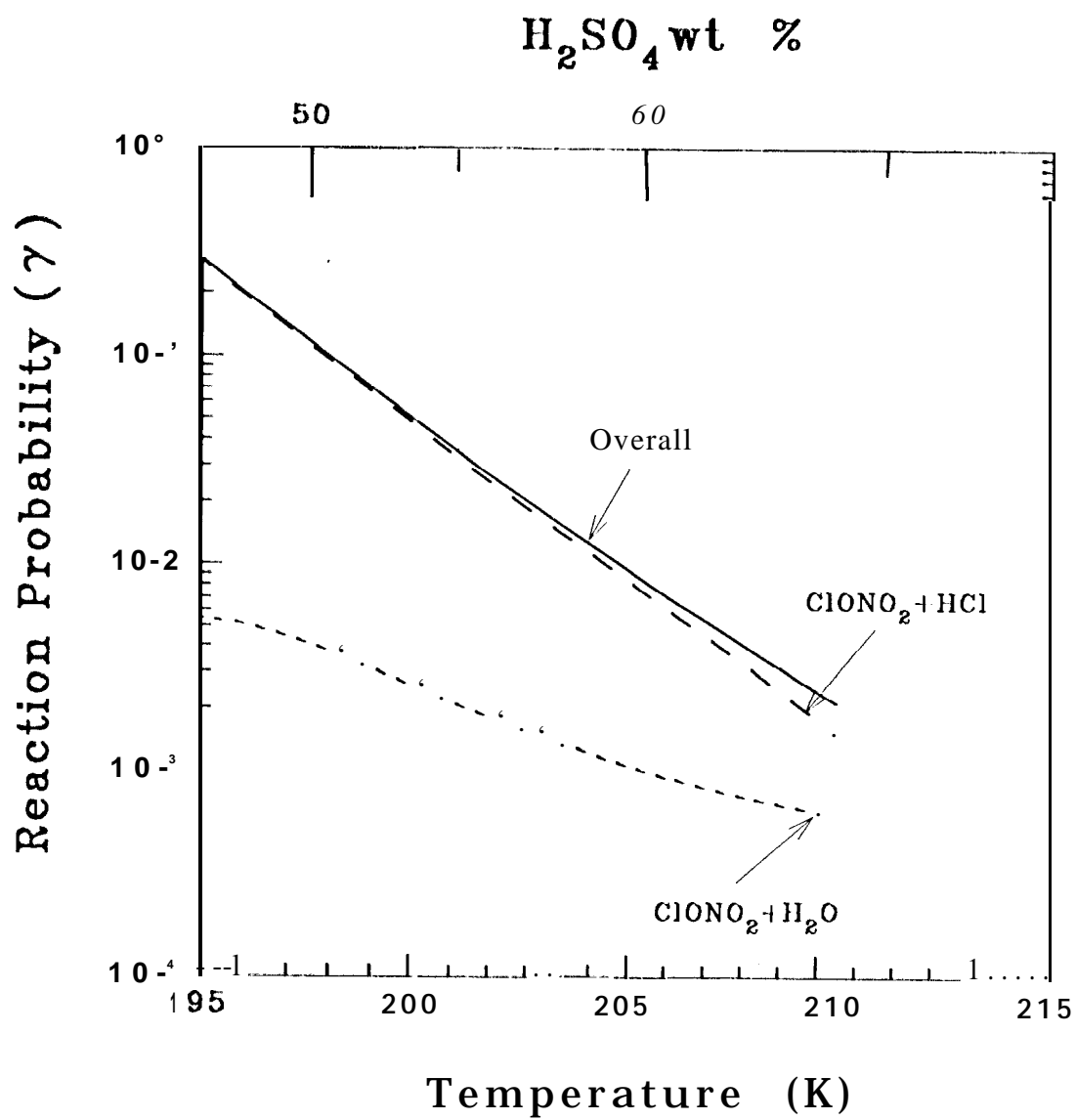


Fig. 22

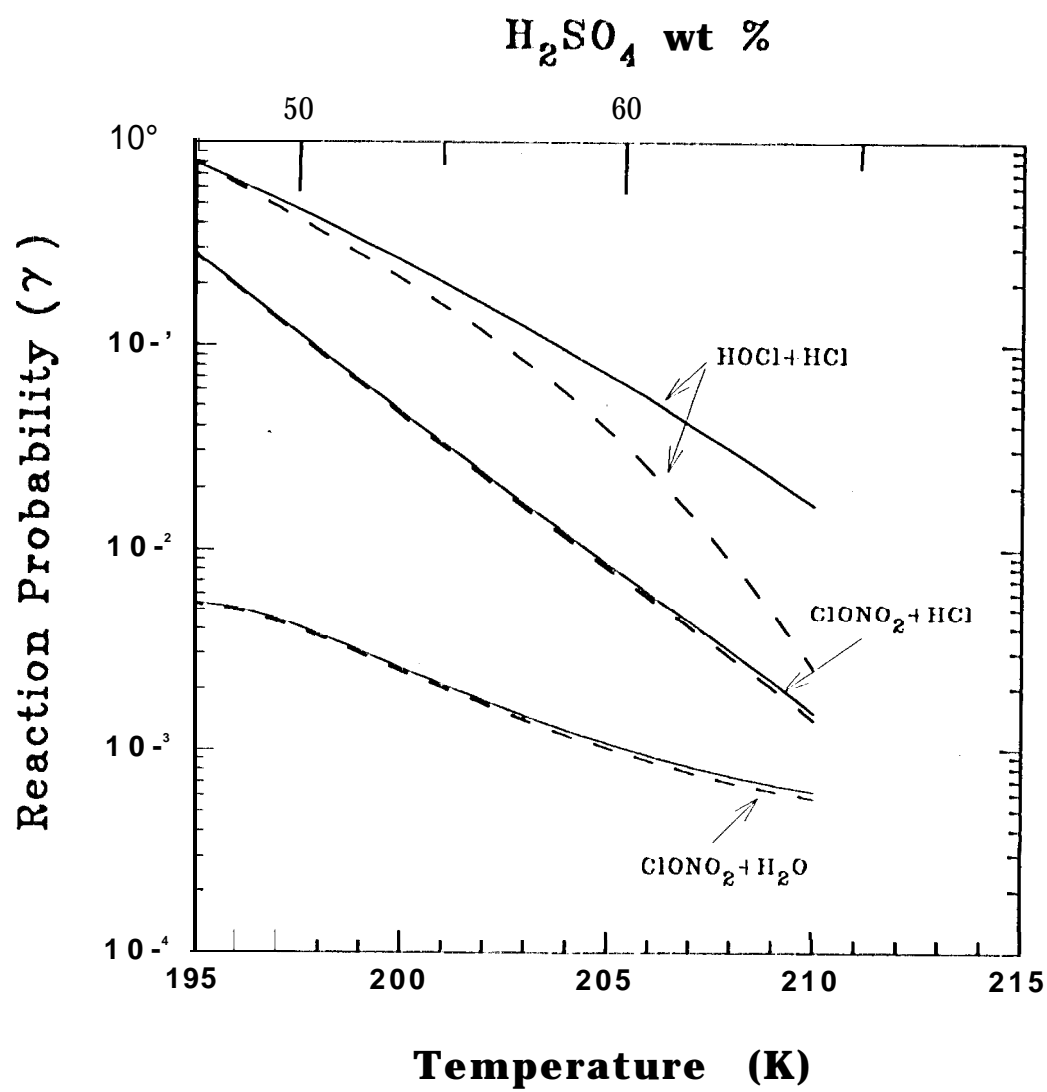


Fig. 23